Two-dimensional supramolecular self-assembly: nanoporous networks on surfaces

Tibor Kudernac, Shengbin Lei, Johannes A. A. W. Elemans and Steven De Feyter*

Received 4th July 2008
First published as an Advance Article on the web 18th November 2008
DOI: 10.1039/b708902n

This *tutorial review* addresses the formation and properties of surface-confined molecular networks as revealed with scanning probe microscopy tools, especially scanning tunneling microscopy. It could be of interest to all interested in surface nano-engineering, and supramolecular chemistry on surfaces. More specifically, this review highlights recent developments in the design of regular nanoporous networks, with a pore diameter ranging from 1 nm to more than 10 nm. The principles leading to their formation are treated in detail and the various functionalities of these porous networks are demonstrated.

1. Introduction

In view of the many possible applications in nanoscience and nanotechnology, controlling substrate composition and functionality is of major interest. As far as control on the nanometer scale (between 1 and 10 nm) is concerned, molecules are the favourite building blocks to decorate, structure, and functionalise surfaces. Following a bottom-up strategy, the tools of supramolecular chemistry provide the guidelines how to design molecular building blocks in order to achieve a balance between molecule–molecule, molecule–substrate, molecule–solvent, and solvent–substrate interactions (Scheme 1) leading to the targeted functional patterns.[1] The reversibility of non-covalent interactions, *i.e.* hydrogen bonding, van der Waals, and metal–ligand interactions to indicate the most popular ones, at the time scale of the self-assembly process guarantees the best possible conditions to achieve equilibrium.[2]

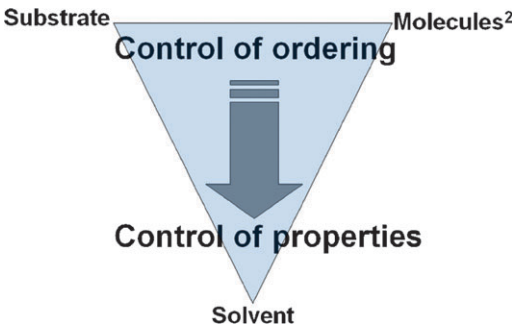

Scheme 1 Interaction scheme at a liquid–solid interface. Under ultrahigh vacuum (UHV) conditions, this scheme simplifies to molecule–molecule and molecule–substrate interactions.

The interaction of alkylthiols with gold is a textbook example of self-assembled monolayers (SAMs).[3] Though the

Department of Chemistry, Laboratory of Photochemistry and Spectroscopy, and INPAC-Institute for Nanoscale Physics and Chemistry, Katholieke Universiteit Leuven, Celestijnenlaan 200-F, 3001 Leuven, Belgium. E-mail: Steven.DeFeyter@chem.kuleuven.be; Tel: (+32) 16-327-990

Tibor Kudernac obtained his PhD in chemistry in 2007 at the University of Groningen (the Netherlands), under the supervision of Prof. B. L. Feringa. His PhD work aimed at investigating the design, synthesis and applications of photochromic molecular switches. He then joined the research group of Prof. S. De Feyter at K. U. Leuven in Belgium, where he investigates self-assembly phenomena at solid–liquid interfaces.

Shengbin Lei obtained his PhD in 2002 in physical chemistry at the Institute of Chemistry, CAS (China) with Prof. Chen Wang. Thereafter he worked first as an assistant and then associate professor at the same institute, in the field of surface assembly and scanning tunnelling microscopy. In 2006, he joined the group of Prof. Steven De Feyter at K. U. Leuven, and works now in the field of 2D nanoporous networks and host–guest chemistry.

Hans Elemans completed his PhD in physical organic chemistry in 2001 with Prof. Roeland J. M. Nolte at the Radboud University Nijmegen (The Netherlands). Since 2003, he occupied a bridging position between the solid-state physics and organic chemistry groups. For this work he was awarded a 'Veni' innovative research grant in 2004. In February 2008 he moved to the group of Prof. Steven De Feyter at K. U. Leuven (Belgium).

Steven De Feyter is professor at K. U. Leuven in Belgium. After starting up scanning tunnelling microscopy during his PhD at K. U. Leuven he moved for a postdoctoral position to the group of Prof. Ahmed Zewail (California Institute of Technology, Pasadena). His current interests include the study of supramolecular chemistry and self-assembly phenomena at surfaces with scanning probe methods with a focus on solid–liquid interfaces.

molecule–substrate interaction is covalent in nature, large scale ordering is achieved leading to crystalline domains, with a lateral periodicity in the order of only 0.5 nm. The sulfur–gold interaction dominates the periodicity of the monolayer and the van der Waals interactions between the alkyl chains, which are at an angle of about 30° with respect to the surface normal, further stabilise the monolayers. The properties of these layers depend on the end groups attached to the alkyl chains. Such layers have useful properties ranging from metal corrosion protection to tuneable wettability of surfaces, to name only a few. These properties heavily depend though on the density of the monolayer. Porosity is detrimental to corrosion protection for instance.

However, certain applications (*vide infra*) ask for functionalised porous surfaces. In this review, we focus on the formation and properties of such surface-confined self-assembled porous molecular systems which often show ordered and crystalline pattern formation with a periodicity up till 10 nm and a pore cavity up till 5 nm or even more. The most popular tools to probe the structure and properties of these layers are about 25 years old. These are the so-called scanning probe techniques, such as scanning tunneling microscopy (STM)[4] and atomic force microscopy (AFM),[5] which often unravel the structural aspects of these films with submolecular resolution. These tools operate under ultrahigh vacuum conditions, ambient conditions, as well as in liquids.

In this review, we will give a brief account on how (supra)-molecular surface-confined pores can be formed, *i.e.* how can the intrinsic non-porous nature of self-assembled monolayers be overcome, their properties and applications. As often, Nature is a source of inspiration. The first part will deal with porous natural systems. The second part deals with the design principles and the formation of porous two-dimensional self-assembled molecular lattices. The third part deals with the properties of these surface-confined porous networks including host–guest chemistry and molecular dynamics.

2. Biomolecular macrocycles

Nature has always been a tremendous source of inspiration for chemists in designing molecular building blocks and functional materials. In living organisms, cyclic structures are widely present at different sizes and complexities, *e.g.* as small porphyrin moieties, which are part of catalytic enzymes, to self-assembled protein complexes of photosynthetic machineries. In such complex biological architectures, the precise organisation of individual components in a superstructure plays an essential role to express a certain function. Specific arrangements and collective properties of molecules within cell membranes can enhance the efficiency of self-assembled biological systems, and therefore it is of great interest to study the topographies of such systems as their understanding could help us to design and construct artificial and functional two-dimensional (2D) materials. AFM is the technique of choice to study biological materials adsorbed on solid substrates, because in contrast to electron microscopy it can be carried out under ambient conditions and a resolution at the sub-nanometre level can be achieved.

2.1 Naturally occurring macrocyclic architectures

Nature creates cyclic architectures for their specific functions rather than for their beauty. For instance, adenosine triphosphate (ATP) synthase motors use the rotation of their cyclic turbine for the synthesis of ATP molecules. The passage of protons through the membrane results in the rotation of membrane-embedded rotating subunits[6] and this circular movement is further translated into conformational changes within the catalytic subunits of the stator, which lead to the synthesis of ATP. The rotating subunits are complexes of identical protein moieties, which are arranged in a cylindrical ring. The number of protein units determines the efficiency of energy conversion and is dependent on the type of organism. Recently, the rotating subunit-III of spinach-chloroplast ATP synthase was isolated and reconstituted (self-assembled) in a bilayer, forming well-ordered 2D arrays at a high protein-to-lipid ratio.[7] Contact-mode AFM was used to visualise the self-assembled arrays of the subunit III (Fig. 1A–E). Two distinct cyclic structures protruding from the lipid bilayer were observed and characterised by their outer diameters of respectively 5.9 and 7.4 nm. The internal voids of 3.5 nm, however, were identical, which was attributed to opposite orientations of the channels with respect to the membrane surface. From a detailed analysis of the cyclic protein oligomers it was concluded that they are composed of 14 symmetrically distributed subunits. AFM thus proves to be a suitable analytical tool for structural analysis of biological materials near to their native conditions.

A careful design of artificial functional multi-component systems by self-assembly is not only important for the outcome of their resulting supramolecular architecture, but also for their functioning. As we learn from Nature, a specific arrangement of the different constituting components will have an effect on the efficiency of the system. An illustrative example of such a perfectly organised self-assembled system in Nature is the photosynthetic apparatus of the bacterium *Rhodospirillum photometricum* in its native membrane, which has been studied with AFM.[8] The remarkably high quantum efficiency of the photosynthetic systems is mainly attributed to a highly specific arrangement of chromophores in 2D circular structures. Initial steps of the photosynthesis are associated with the light-harvesting pigment-protein complexes LH1 and LH2, which harvest light and channel its energy cascade-wise towards the reaction centre (RC) where it is converted into an electrochemical potential. With AFM, cyclic structures with two different sizes were visualised, of which the smaller are composed of nine subunits and are identified as the LH2 complexes, and the larger as LH1 complexes (Fig. 1F–H). The latter have a slightly ellipsoidal shape and host an RC complex. The distribution of the LH1 and LH2 complexes is not random because a significant clustering of both the LH1 complexes hosting the RCs, and of LH2 complexes was observed. On the other hand, a complete phase separation does not occur, and thus a short distance between the LH2 complexes and a LH1-RC complex is always ensured. It is hypothesised, that such an arrangement offers an ideal balance between short distances for the diffusion of excitation energy to the closest RC, and a possible further diffusion to a closely

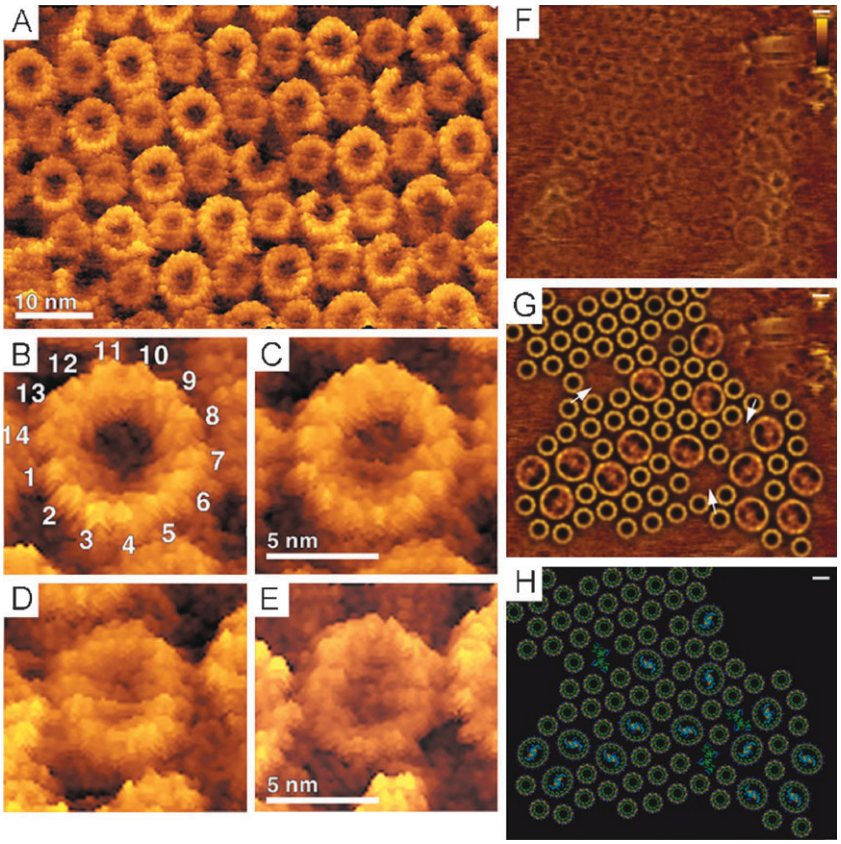

Fig. 1 (A–E) Subunit-III oligomers of chloroplast ATP synthase visualised by AFM. (A) 2D arrays of the subunit-III at high protein-to-lipid ratio with the distinct wide (B–C) and narrow (D–E) rings, which is attributed to the two different orientations with respect to the surface. (Reproduced with permission from ref. 7. Copyright 2000 Nature Publishing Group.) (F–H) AFM images of the photosynthetic apparatus of a native chromatophore membrane. (F) Raw AFM data. (G) Fitting of the LH2 and core-complex averages corresponding to the relative positions and orientations in the topograph. (H) Model of the LH2 structures and the core-complexes based on the topograph. (Reproduced with permission from ref. 8. Copyright 2004, National Academy of Sciences.)

positioned RC that is active at the time, in case that the previous RC was in its inactive phase. As the distribution of the large and small rings is not random, there must be some preference for the individual components to interact with each other. However, the lack of complete phase separation suggests that the differences in energy of these interactions are rather subtle. It will be a great challenge to rationally design and construct such 2D artificial assemblies in the laboratory, but nevertheless they might be of great importance as is demonstrated by the high efficiency of the natural photosynthetic systems.

2.2 Self-assembly of DNA into macrocyclic structures

DNA is an excellent example of a molecular recognition system. Two complementary strands are linked together *via* non-covalent interactions into a one-dimensional (1D) double helix. This highly selective recognition, which is mainly governed by highly specific and directional hydrogen bonding interactions between the DNA base pairs, can also be utilised in nanotechnology to construct predictable self-assembled architectures.[9] A common strategy to construct DNA complexes is to use so-called ''sticky ends'': short, single-stranded sequences of nucleotide bases that protrude from the terminus of a double-stranded DNA helix. If another DNA molecule with a complementary single-stranded sequence is present, the two molecules will self-assemble to form a supramolecular complex. A limitation of this approach is that due to the 1D character of unbranched double-stranded DNA, the complexity of potential products is limited since only linear structures are being formed. In order to create two-dimensional architectures, multicomponent systems should be employed which are based on more complex single-stranded DNA motifs. As an example, a three-point-star DNA motif with a three-fold rotational symmetry was assembled from seven DNA single strands (Fig. 2A–B).[10] When the side-arms are terminated with sticky ends, the DNA ''stars'' self-assemble into porous, hexagonal arrays. Because of the three-fold rotational symmetry of the motif, the same sticky ends are present on every side-arm, and this ensures the same strength of interactions in all three directions, resulting in an isotropic growth of the assembly. The hexagonal 2D crystalline arrays of such DNA motifs were highly ordered, as was judged from Fourier transform analysis of the AFM images (Fig. 2B). The diameter of the pores was approximately 30 nm. The commonly observed problem observed for lattices that are self-assembled from DNA motifs, is that only relatively small domains are formed with sizes that are typically smaller than

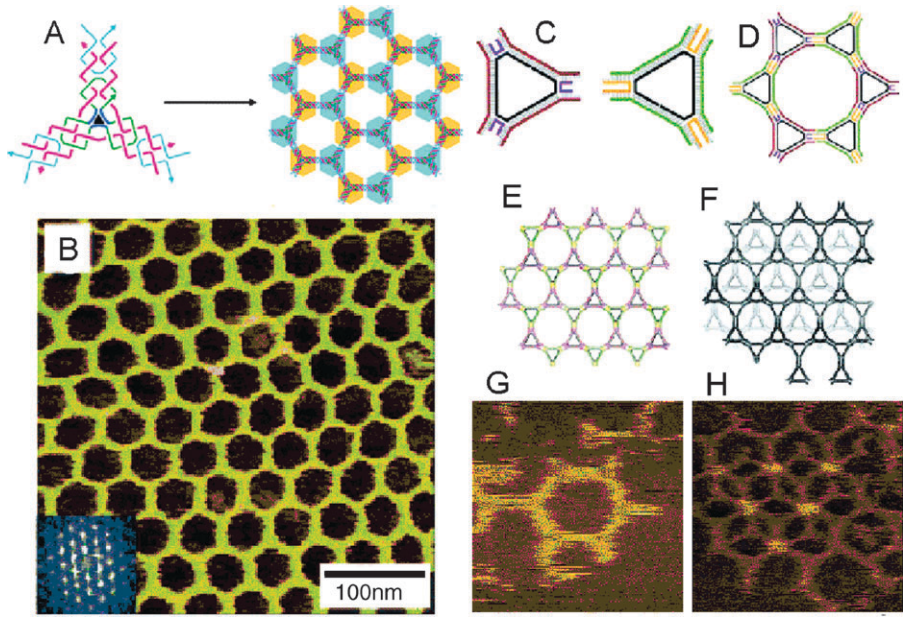

Fig. 2 (A) Schematic representation of three-point-star DNA motifs that assemble into hexagonal 2D crystalline DNA arrays *via* sticky ends. (B) AFM image of such a self-assembled pattern; the inset is a corresponding Fourier transform pattern of the hexagonal DNA array. (C) Schematic representation of the two types of triangular DNA complexes that can connect to each other by complementary base pairing. (D) Hexagonal structure composed of six triangular complexes. (E) 2D hexagonal array composed of hexagonal structures. (F) A pair of overlapping 2D arrays. Top layer shown black; bottom layer shown grey. (G) AFM image of a hexagonal structure composed of six triangular complexes. (H) AFM image of a pair of overlapping hexagonal 2D DNA arrays. (Reproduced with permission from refs. 10 and 11. Copyright 2005 and 2004, American Chemical Society.)

1 μm. However, in the case of the three-point-star motif, domains of self-assembled DNA arrays as large as 1 mm were found.

In another approach towards constructing macrocyclic arrays, two types of pre-constructed triangular DNA complexes, both composed of seven strands, were self-assembled at room temperature into hexagonal lattices and visualised with AFM (Fig. 2C–H).[11] Unpaired complementary bases at their vertices were designed to stick to one another, thus allowing the triangles to connect at these sticky ends. Fig. 2G shows a single macrocyclic hexagon with an internal diameter of 35 nm. Besides individual hexagons, small but regular hexagonal domains can be observed. In the AFM image in Fig. 2H, two hexagonal domains are present which are positioned on top of each other, and in which one half of the triangles of the upper domain lies in the centres of the hexagons of the bottom domain and the remaining triangles directly on top of other triangles. Such an offset arrangement appears to be the most stable one, probably as a result of favourable interactions between the triangles of the upper layer and the substrate. Indeed, the AFM images reveal greater heights at points where the triangles overlap, whereas the remaining areas seem to have similar contrast.

3. Covalent nanoporous networks

Although Nature has provided us with several beautiful examples of porous and circular architectures, their tremendous complexity, which is a result of billions of years of evolution, prevents their artificial construction in the laboratory. However, a practical alternative is to use Nature's examples as a blueprint, and design and synthesise simplified artificial porous structures by standard chemical procedures. At first sight, a logical approach to do this is to synthesise circular molecules that contain a cavity, and adsorb them onto a surface. Amongst the simplest covalent cavity molecules are crown ethers, which have a circular structure containing polar groups that are directed to the interior of the crown, so that they are perfectly preorganised to bind cationic guests such as alkali metal ions. As a result of their generally flat structure, crown ethers are ideal candidates for constructing nanoporous networks at a surface. Indeed, self-assembled monolayers of dibenzo-18-crown-6[12] and tetracrown ether-functionalised phthalocyanines[13] have been successfully adsorbed to a solid–liquid interface in an electrochemical STM (EC-STM), and their binding of potassium and calcium ions, respectively, could be imaged at the submolecular level. Other flat, cavity-containing molecules, such as shape-persistent organic macrocycles, appeared to form nanoporous networks with pore sizes of $\sim$2 nm.[14] Crown-shaped molecules with a more three-dimensional structure have also been used to create networks with large pores. The bowl-shaped calix[8]arene host shown in Fig. 3A has a cavity which is so large that it can accommodate big guest molecules, such as fullerenes, in its interior (Fig. 3B).[15] In EC-STM images of monolayers of the calix[8]arenes at the interface of Au(111) and aqueous 0.1 M $HClO_4$, dark depressions are observed which can be associated with the cavities of the hosts (Fig. 3C). Monolayers of the hosts with fullerene molecules bound in their cavities at the same interface showed similar patterns in the STM image, but

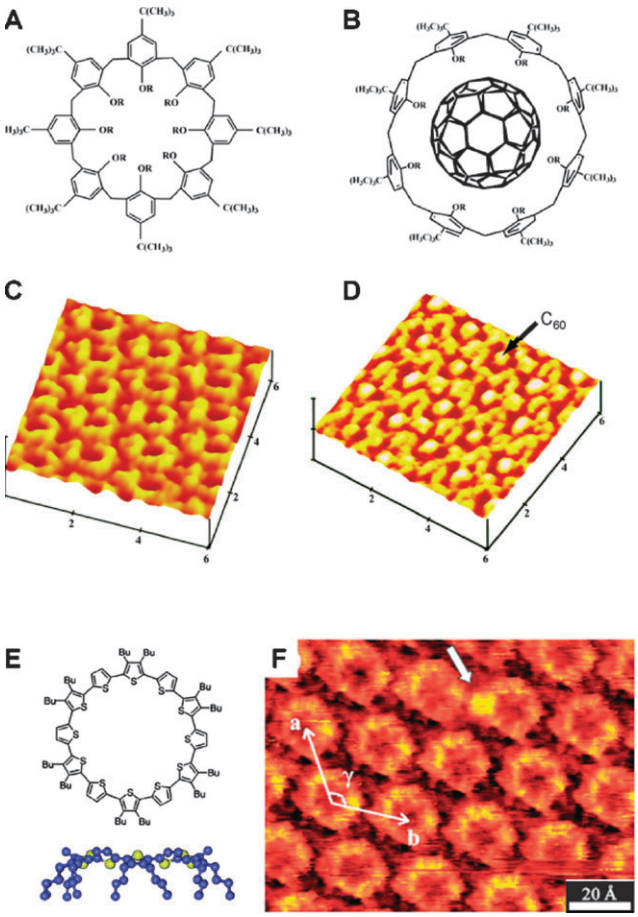

Fig. 3 (A) Molecular structure of a calix[8]arene host. (B) Schematic representation of the host–guest complex between the calix[8]arene and a fullerene. (C) EC-STM image of a monolayer of the hosts at the interface of Au(111) and 0.1 M $HClO_4$. (D) *Idem*, of a monolayer of the host–guest complex with C_{60}; The arrow points at a bound fullerene molecule. (E) Molecular structure of a cyclo[12]thiophene and its spider-like conformation at a graphite surface. (F) STM image of cyclo[12]thiophenes at the interface of graphite and 1,2,4-trichlorobenzene. The arrow points at a C_{60} molecule that is bound at the rim of one of the macrocycles. (Reproduced with permission from refs. 15 and 16. Copyright Wiley-VCH Verlag GmbH and Co. KGaA.)

bound C_{60} guest molecules are now clearly identifiable as bright spots in the centres of the cavities (Fig. 3D).

In another example, fully conjugated cyclo[12]thiophenes self-assembled at a graphite surface into porous networks, in which the macrocycles adopt a spider-like conformation. As a result their aromatic rings are positioned approximately 0.5 nm above the surface (Fig. 3E–F).[16] Upon the addition of a solution of C_{60} to such a network, the fullerene molecules appeared to preferentially bind on top of the rim of the cyclo[12]thiophenes.[17] Occasionally, they are also captured within the pores, but in that case their binding was found to be very labile. At the rims, their binding is stabilised by attractive donor–acceptor interactions between the electron-rich thiophenes and the electron–deficient fullerenes. Irrespective of the multiple binding sites on each cyclothiophene, exclusively 1 : 1 complexes were formed, because upon binding of a fullerene the HOMO of the underlying macrocycle shifts drastically towards the binding site, thereby creating a dipole which disfavours the complexation of additional fullerenes. In addition, due to the close proximity of the macrocyclic backbones in the monolayer (<0.4 nm), this dipole induces a quadrupole in adjacent macrocycles and as a result at higher concentration of the additive, monolayers fully covered with C_{60} molecules are formed in which they bind to the underlying cyclothiophenes at exactly the same positions.

At first sight, the concept of constructing well-defined nanoporous networks simply by depositing pre-constructed cavity-containing molecules onto a surface might look appealing, but when these molecules start to adopt a more three-dimensional structure, it is not always trivial to control their orientation upon deposition. If they become oriented in a specific packing, which for example hinders or prevents access to their cavities, the desired application of the resulting 2D

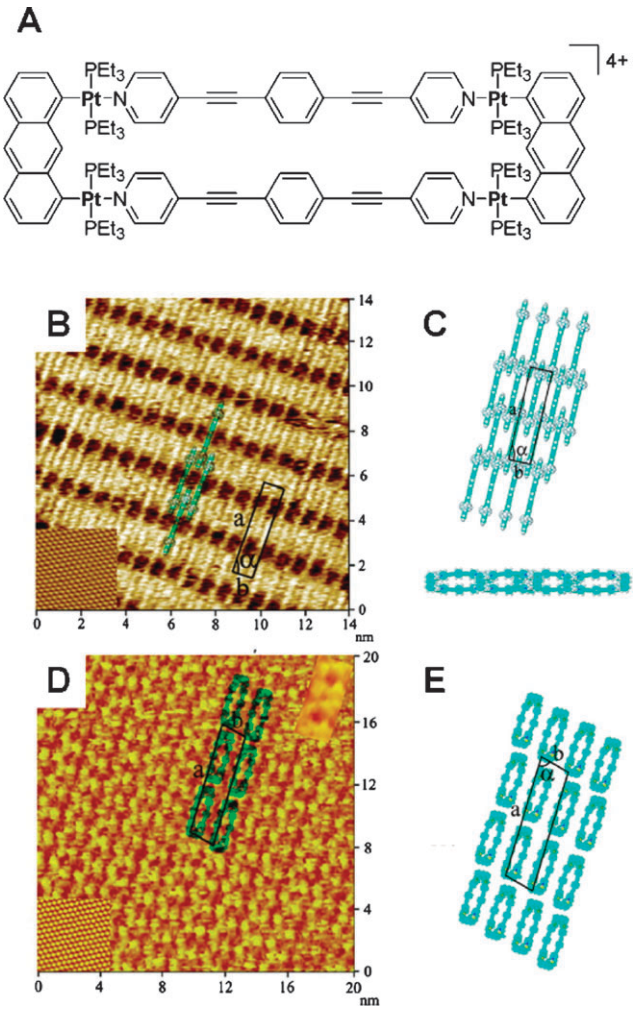

Fig. 4 (A) Structure of a supramolecular rectangle. (B) STM image of a monolayer of the rectangles at a graphite-air interface (inset in left bottom corner: STM image of graphite). (C) Molecular models (top and side view) illustrating the 'edge-on' orientation of the rectangles on graphite. (D) EC-STM image of a monolayer of the rectangles at an interface of Au(111) and a 0.1 M $HClO_4$ solution in water. (E) Molecular model illustrating the 'face-on' orientation of the rectangles on Au(111). (Reproduced with permission from ref. 18. Copyright 2005, National Academy of Sciences.)

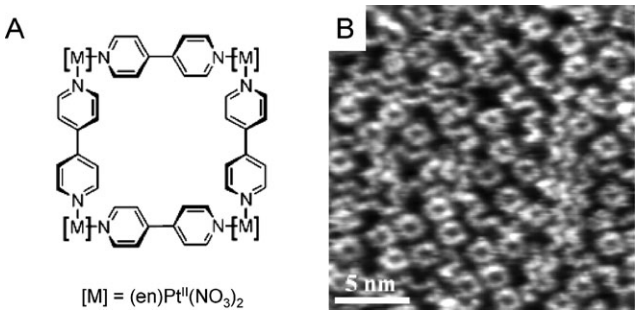

Fig. 5 (A) Structure of a supramolecular square. (B) EC-STM image of a monolayer of the squares at the interface of a Cl-modified Cu(100) surface and an aqueous HCl/KCl solution. (Reproduced with permission from ref. 19. Copyright Wiley-VCH Verlag GmbH and Co. KGaA.)

nanoporous surface might be completely lost. It should be realised that already the nature of the surface on which the molecules are deposited can play a detrimental role in their orientation. For example, at a graphite surface, the supramolecular rectangles shown in Fig. 4 self-assemble in an 'edge-on' geometry in which their cavities are not exposed to the STM tip.[18] In contrast, at a Au(111) surface the same molecules self-assemble in a 'face-on' geometry, with their cavities now oriented towards the STM tip. The difference in orientation finds its origin in a difference in interaction strength between the surface and these particular molecules. On graphite, this interaction is relatively weak and as a result intermolecular interactions dominate the self-assembly, resulting in the 'edge-on' orientation of molecules. On gold, the interaction between the surface and the molecules is much stronger and leads to a completely different orientation of the cavities.

Ideally, one would like to have complete control over the properties of the underlying surface. An elegant approach to get such control is to modify the surface in such a way that a desired orientation of the adsorbing molecules is specifically induced. This approach was used to deposit supramolecular squares, with four positively charged Pt^{2+} corners, onto a Cu(100) surface in a 'face-on' geometry, *i.e.*, with their cavities exposed to the STM tip.[19] It was reasoned that such an orientation could be induced by enhancing the interactions between the surface and the positive charges of the molecules. In order to accomplish this effect, a negatively charged layer of chloride anions was deposited onto a positively polarised Cu(100) electrode. In a subsequent adsorption step, the metallo-squares were adsorbed under potential control onto the templating surface, and indeed patterns of porous molecules, which all have their cavity exposed to the STM tip, were obtained (Fig. 5).

4. Self-assembled nanoporous networks

Although the examples in the previous section have shown that constructing a nanoporous network by depositing preformed cavity molecules onto a surface can be quite successful, an important limitation of this approach remains in many cases their time-consuming and generally complex synthesis. In relation to this, the introduction of desired modifications of the cavity molecules is often far from straightforward. An alternative to using covalently built cavities is to generate hosts *in situ* at the surface during the adsorption process, by means of supramolecular self-assembly of small complementary components that are relatively easy to synthesise. In three dimensions, self-assembly of discrete, porous architectures is often elusive, due to unpredictable entropic factors that can play a role when many components have to be brought together into one well-defined structure. However, at a surface or interface, the confinement of these components to two dimensions already eliminates several degrees of translational, rotational and vibrational freedom. In addition, network formation by supramolecular interactions should ideally be under thermodynamic control and thus display a high degree of self-repair, so that finally defect-free assemblies are obtained. 2D nanoporous networks at a surface can be generated by means of several types of supramolecular interactions, *e.g.*, hydrogen bond-directed

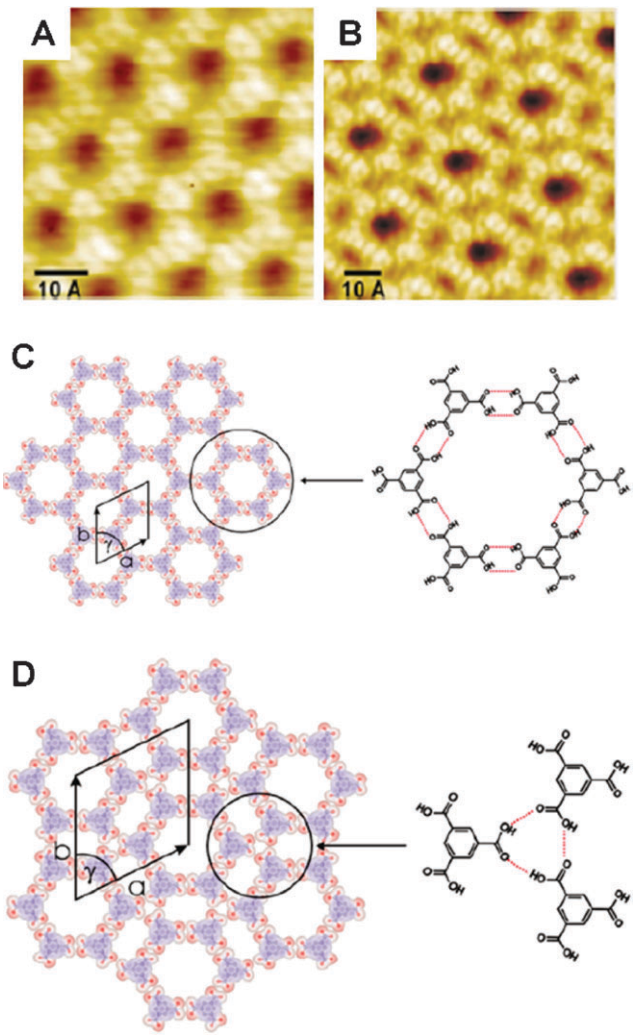

Fig. 6 (A) UHV STM images of the honeycomb network formed by TMA on graphite. (B) *Idem*, of the flower network. (C) Molecular model of the honeycomb structure. (D) *Idem*, of the flower structure. (Reproduced with permission from ref. 21. Copyright Wiley-VCH Verlag GmbH and Co. KGaA.)

homo- and hetero-assembly of organic molecules, the coordination of metal centres to organic ligands, surface dewetting, dipole–dipole, van der Waals, or a combination of several of the interactions.

4.1 Supramolecular interactions to form nanoporous networks

A pioneering example of a nanoporous self-assembled network, which is formed both in UHV[20] and at solid–liquid interfaces,[21] is based on hydrogen bonding interactions between trimesic acid (TMA, 1,3,5-benzenetricarboxylic acid) building blocks. As a result of the planar structure of the molecule and the positioning of the trigonal exodentate functional groups, in most cases on a surface porous networks are being formed through dimerisation of the carboxylic acid groups. In UHV on graphite, mainly two phases are found which are referred to as the "chicken-wire" or "honeycomb", and the "flower" structure (Fig. 6A and B). In the honeycomb structure, each pore is surrounded by six TMA molecules which are all connected *via* double hydrogen bonding interactions between the carboxylic acids (Fig. 6C). In the flower structure, the TMA molecules are arranged in similar 6-fold rings, but these rings are more closely packed. In contrast to the honeycomb structure, where one of the carboxylic acid groups of each TMA molecule actively participates in the hydrogen-bonding seam of a neighbouring ring of the network, it serves here as a bridge to two neighbouring rings *via* a three-point interaction with two adjacent carboxylic acid groups (Fig. 6D). As such, the flower structure can be considered a closely packed variant of the honeycomb structure.

Also derivatives of TMA, such as 1,3,5-tris(10-carboxydecyloxy)-benzene (TCDB), can form extended networks.[22] On graphite, this molecule, which has three long aliphatic C_{10}-spacers between the core and the hydrogen-bonding functionalities, forms a pseudo-rectangular network in which two of the carboxylic acid groups of each molecule form hydrogen bonds with a neighbouring molecule to form a pore, whereas the third carboxylic acid dimerises *via* hydrogen bonds with the carboxylic acid of a more distant TCDB molecule (see section 5.1). This example perfectly illustrates that simple modifications in a molecule, which is encoded to form a network by self-assembly through specific supramolecular interactions, can afford a certain degree of control over the resulting pore size.

The self-assembled networks based on TMA and TCDB still have relatively small pore sizes, comparable to the size of a single component of the arrays that line the pores. An approach that has been successfully applied to increase pore size is to use two components, which for example interact *via* highly directional hydrogen bonding interactions. In an illustrative example, melamine, a molecule with three-fold symmetry, was co-adsorbed together with perylene tetracarboxylic diimide (PTCDI) onto a silver-terminated silicon surface in UHV.[23] A hexagonal network with pores having a size of $\sim$2 nm was formed, in which the melamine molecules serve as the junctions and the PTCDI molecules as the sides (Fig. 7). The success of this approach relies on the choice of hydrogen bonding interactions: melamine and PTCDI were chosen because they are expected to interact much more strongly by means of hetero- as opposed to homo-molecular

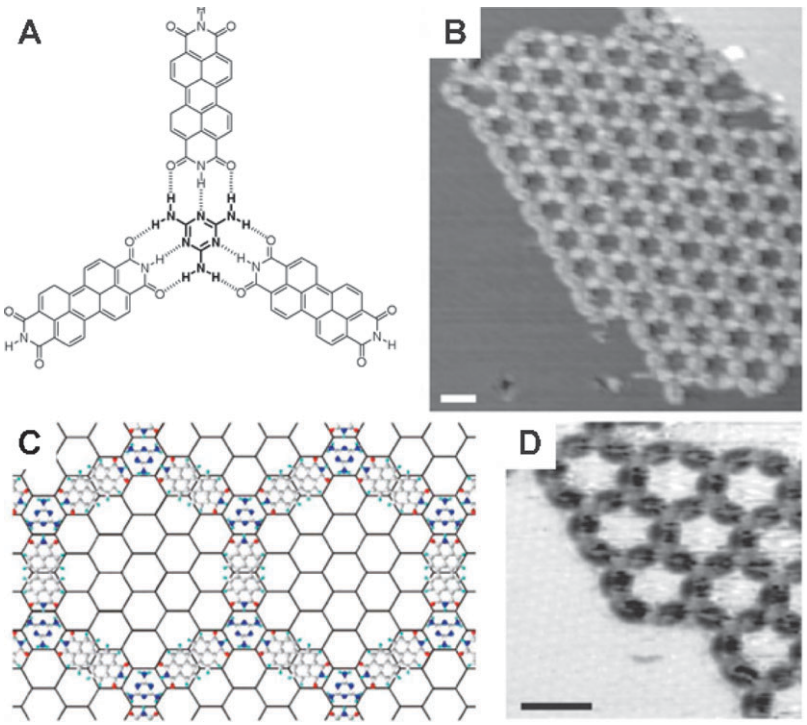

Fig. 7 (A) Molecular arrangement of melamine (bold) and PTCDI in a hydrogen-bonded junction of the network. (B) UHV STM image of a melamine–PDCTI network on a silver-terminated silicon surface; scale bar is 3 nm. (C) Schematic diagram in which the registry of the network with respect to the surface is shown. (D) UHV STM magnification of the network at inverted contrast; scale bar is 3 nm. (Reproduced with permission from ref. 23. Copyright 2003, Nature Publishing Group.)

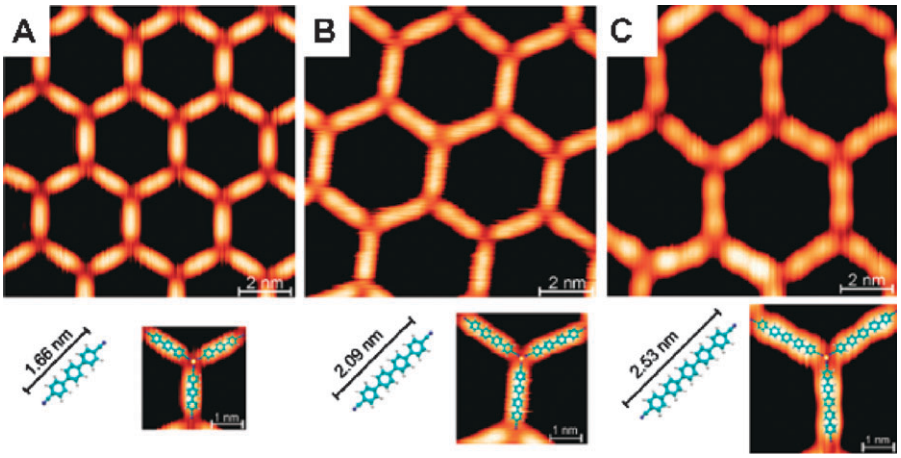

Fig. 8 UHV STM images of the Co-directed self-assembly of (A) NC-Ph_3-CN, (B) NC-Ph_4-CN, and (C) NC-Ph_5-CN on a Ag(111) surface. Underneath the STM images, molecular models of the ligands and their superposition onto the STM images are depicted. (Reproduced with permission from ref. 24. Copyright 2007, American Chemical Society.)

hydrogen bonding, which is attributed to the fact that a complementary melamine–PTCDI pair self-assembles *via* three hydrogen bonds, as compared with just two in the case of homo-molecular pairs.

Instead of hydrogen bonding interactions, also metal–ligand coordination chemistry can be applied to construct bicomponent networks. In this approach, transition metal centres are used to connect two or more organic ligands by highly specific and directional interactions. By making use of specific metal–ligand combinations, many parameters of the resulting architectures, such as binding stoichiometry, angle, strength, and reversibility, can be controlled and predicted.

Metal–ligand coordination between cobalt atoms and ditopic dicarbonitrile polyphenyl (NC-Ph_n-CN) organic linkers has led to the development of a highly open surface-confined nano-mesh realised by 2D self-assembly.[24] In a two-step procedure in a UHV STM, first the ligands were evaporated onto a Ag(111) surface, followed by cobalt atoms to construct the 2D network *in situ*. By using ligands with different length, huge domains ($>\mu m^2$) of hexagonal porous networks can be obtained with tuneable pore dimensions. In the case of the NC-Ph_5-CN linker, their size can be up to 5.7 nm (Fig. 8). A remarkable aspect of these networks is that the cobalt centres bind three ligands, which is uncommon for cobalt–carbonitrile complexes in the bulk. DFT calculations afforded evidence that the underlying Ag(111) surface plays an essential role in this coordination stoichiometry, in the sense that the presence of a metal–metal bond between a cobalt and a silver atom strongly determines the number of organic ligands that can still bind to the cobalt centre.

Recently it has been shown that networks with very large pores can also be formed from a single component system, albeit by means of supramolecular interactions that *a priori* are rather difficult to predict. UHV STM studies revealed that upon depositing anthraquinone molecules onto a Cu(111) surface, a honeycomb network was formed in which each of the pores is lined by 18 molecules, defining a pore size of $\sim$5 nm with each of the pores enclosing more than 200 uncovered copper atoms (Fig. 9).[25] Detailed analysis of the

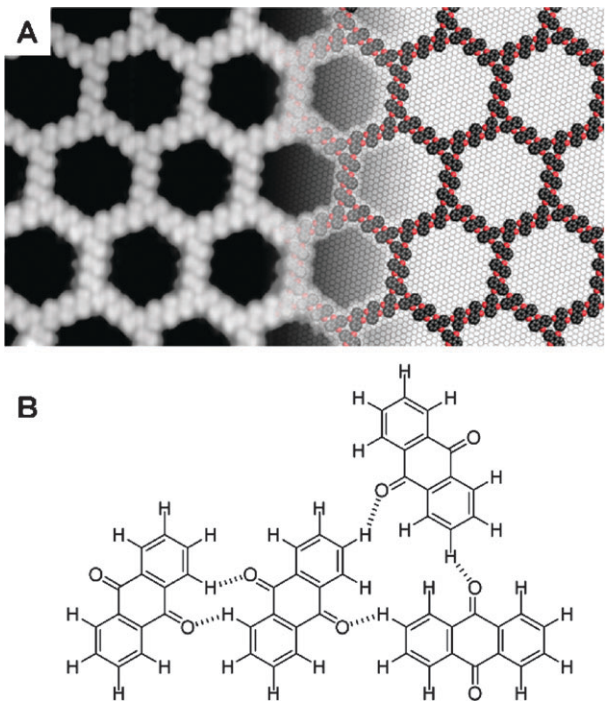

Fig. 9 (A) UHV STM image (26 × 15 nm) of the honeycomb network formed by anthraquinone molecules at a Cu(111) surface; in the right part of the image, a modelled representation of the surface and the adsorbed molecules is drawn in. (B) Molecular arrangement of the self-assembled anthraquinone molecules forming a row (left) and a vertex (right). (Reproduced with permission from ref. 25. Copyright 2006, American Association for the Advancement of Science (AAAS).)

STM images in combination with molecular modelling indicated that the molecules in the hexagons self-assembled *via* C–H$\cdots$O hydrogen bonding interactions between the carbonyl groups and protons coupled to the arene rings of neighbouring molecules (Fig. 9B). The vertices of the honeycomb network are formed by a hydrogen-bonded self-assembled trimer of

anthraquinone molecules. Although these supramolecular interactions can explain the self-assembly into hexagonal networks, it does not explain why each of the hexagon sides consists of exactly three anthraquinone molecules. At low surface coverage, hardly any trimers were found and instead only linear arrays of often several tens of self-assembled molecules. A key observation was that parallel arrays almost never run in close proximity (<5 nm) to one another. This suggests that in addition to attractive hydrogen bonding interactions, also long-range repulsive interactions play a role in the self-assembly. At low coverage these repulsive interactions prevent the formation of trimers and multimers and favour the self-assembly of the molecules in rows, while at higher coverage they prevent the formation of closely packed parallel arrays in favour of a more even distribution of adsorbates that is afforded by their assembly in a honeycomb pattern. In principle, if one could engineer this balance between attractive and repulsive forces, for example by tailoring the molecules with specific functional groups, it should become possible to control the pore size of 2D surface assemblies.

In many cases, an outcome of self-assembly of molecules into organised structures mediated purely by van der Waals or dipole–dipole interactions is difficult to predict because these interactions are less directional than hydrogen bonding and metal–ligand coordination. An illustrative example is the nanoporous network constructed by the self-assembly of porphyrins with two *meso*-(3,5-di-*tert*-butyl)phenyl and two *meso*-3-cyanophenyl groups at a Ag(111) surface, which is governed by a combination of dipole–dipole and van der Waals interactions.[26] In the highly organised network that is formed, the porphyrins are organised in trimeric units in which the cyanophenyl functions are directed towards the pores (Fig. 10). In addition to intermolecular interactions, it was also believed that interactions between the cyano groups and

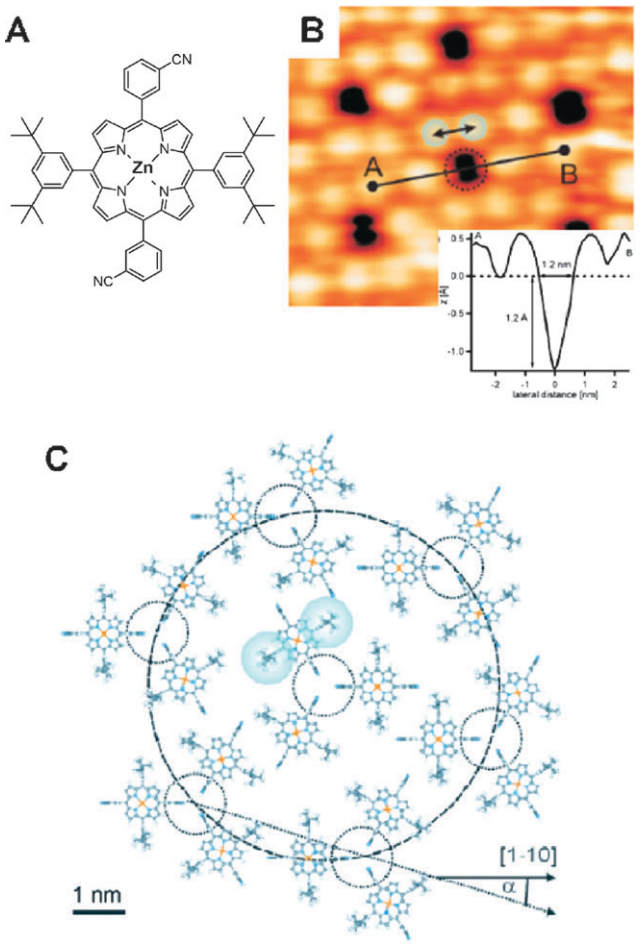

Fig. 10 (A) Molecular structure of a porphyrin with two *meso*-(3,5-di-*tert*-butyl)phenyl and two *meso*-4-cyanophenyl groups. (B) UHV STM image (9.1 × 8.0 nm) of the porous network formed by this porphyrin at a Ag(111) surface; inset: cross section. (C) Model proposed for the self-assembled network. (Reproduced with permission from ref. 26. Copyright Wiley-VCH Verlag GmbH and Co. KGaA.)

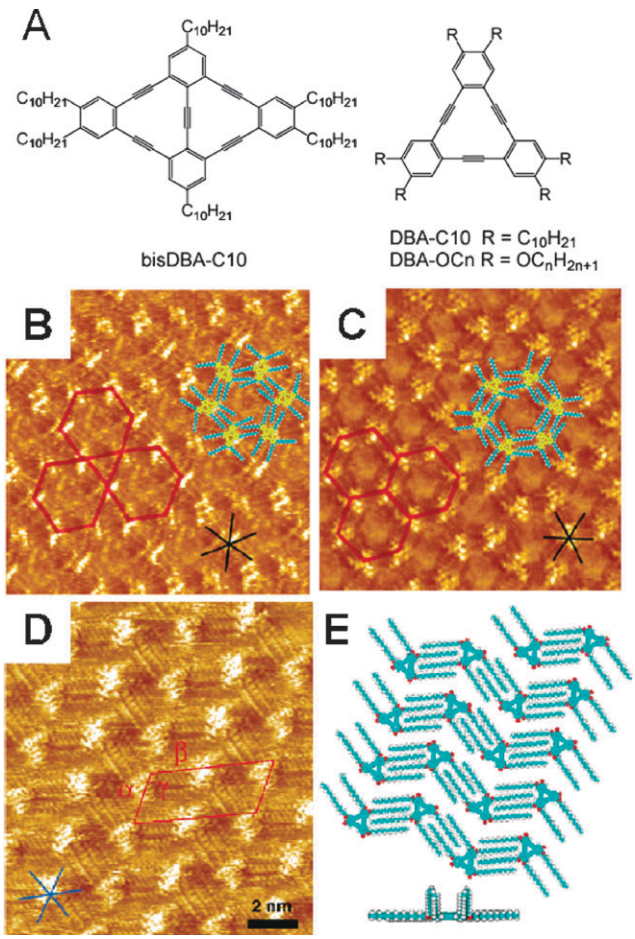

Fig. 11 (A) Molecular structures of a rhomb-shaped bisDBA-C10 (left) and triangular DBAs (right). (B) STM image (20 × 20 nm) showing the Kagomé network formed by bisDBA-C10 at the interface of graphite and TCB. (C) STM image (18.7 × 18.7 nm) of the honeycomb network formed by DBA-C10 at the same interface. (D) STM image of the linear assembly formed by DBA-OC14 at the same interface. (E) Molecular models showing the arrangement of the linear assembly; in the bottom a side-view of one molecule, with two of its alkoxy chains sticking in the liquid, is depicted. (Reproduced with permission from refs. 27 and 28. Copyright 2006, American Chemical Society.)

the underlying silver lattice play a significant role in the final structure of the monolayer.

Alkyl chain interdigitation is one of the most commonly encountered motifs of organised self-assembled monolayers of organic molecules on a surface. It has been proven to be an extremely important interaction for stabilising monolayers in a 2D arrangement, not only by means of interdigitation but also by van der Waals interactions between the surface and the alkyl chains running parallel to it. Because of the structural matching, in particular graphite surfaces interact strongly with such chains, and the strength of the molecule–substrate interactions can generally be controlled by varying their length. In many cases they are observed to orient themselves along one of the symmetry axes of the underlying surface, and it is this directionality that has been used as a tool to systematically study porous network formation based on alkyl-substituted dehydrobenzo[12]annulene (DBA) derivatives (Fig. 11A).[27] The self-assembly of two sets of DBA derivatives with different core shapes, triangular and rhombic, was investigated at interfaces of graphite and a variety of solvents. At the interface of graphite and 1,2,4-trichlorobenzene (TCB), the rhombic bisDBA-C10 self-assembled into a rarely observed Kagomé network (Fig. 11B), while the triangular DBA-C10 formed a honeycomb structure (Fig. 11C). Not only the difference in core shape, but also the location and orientation of the interdigitating alkyl chains play an essential role in the outcome of these 2D structures. It is therefore no surprise that the position at which they are attached to the core, as well as their length, are important parameters. Indeed, upon elongation of the chains, a transition from honeycomb networks to densely-packed linear assemblies was observed (Fig. 11D).[28] In the case of DBA-OC12 and DBA-OC14, coexisting phases were occasionally observed, but for the DBAs with longer alkoxy chains the linear assemblies were exclusively formed. Close inspection of these assemblies revealed that only 4 of the 6 alkyl chains of each DBA molecule were observed in the STM image, which suggests that the other two chains are not adsorbed to the graphite but exposed to the liquid phase (Fig. 11E). A fine balance between adsorbate–adsorbate interactions and adsorbate–substrate interactions is proposed to govern the formation of either honeycomb networks or linear assemblies. The latter are formed because of increasingly enhanced interactions between the elongating alkoxy chains and the graphite surface, and become energetically more favourable than honeycomb networks in which large open voids are present. As an extension of the research it turned out that the energy differences between the surface morphologies were so small that they could be easily tuned by varying the concentration of the DBAs in the subphase, or by the addition of guest molecules with the same shape and size as the voids of the honeycomb network (see section 4).

An even less predictable and in many cases elusive approach to construct porous architectures is to make use of dewetting of thin films of a solution of molecules. As an example, when chloroform solutions of cyclic porphyrin oligomers were drop-casted onto a mica or glass substrate, micrometer-sized rings formed upon evaporation of the solvent (Fig. 12).[29] Their sizes and size distribution could be controlled by adjusting the wettability of the surface. The formation of such well-defined rings is proposed to occur according to the so-called 'pinhole'-mechanism, which is a combined process of molecular self-assembly and physical wetting/dewetting phenomena (Fig. 12D). Upon evaporation of the thin solvent film, at a certain moment pinholes, in which the surface is in contact with air, are formed. At the edges of these pinholes, the rate of solvent evaporation is higher than in other locations in the film, which leads to a flow of solutes in the direction of the pinholes where their concentration locally increases and the material finally accumulates. As a result rings are formed

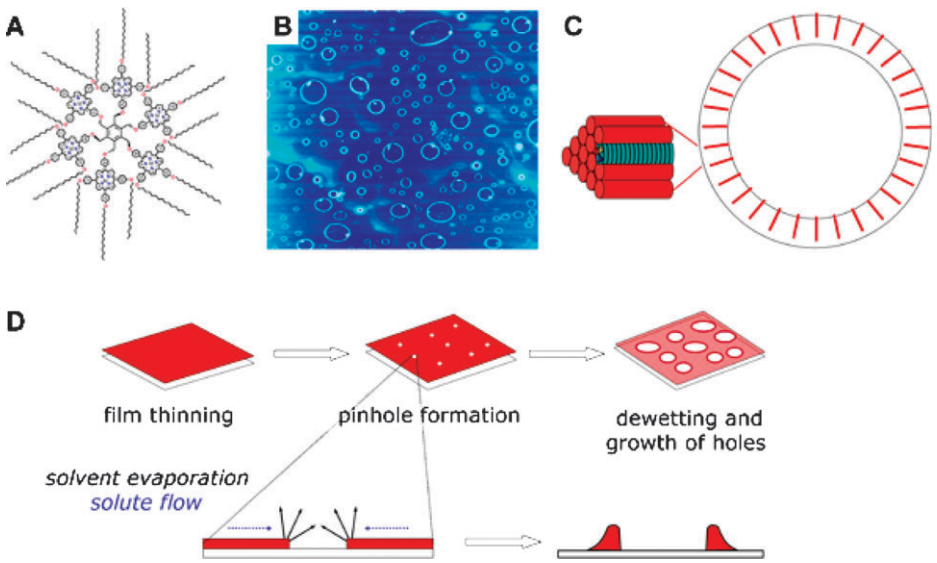

Fig. 12 (A) Molecular structure of a cyclic porphyrin oligomer containing six porphyrins connected to a central benzene core. (B) AFM image (55 × 50 μm) of rings formed after evaporation of a chloroform solution of the porphyrin oligomer on hydrophilic carbon-coated glass. (C) Proposed arrangement of the porphyrin oligomers within the rings. (D) Cartoon representing the pinhole-mechanism of dewetting of a thin film containing solutes.

with an empty interior. Polarised fluorescence spectroscopy and Near field Scanning Optical Microscopy (NSOM) studies revealed that within the rings the porphyrins are organised *via* π–π stacking in 'edge-on' positioned columnar stacks, which are oriented radially within the rings (Fig. 12C).

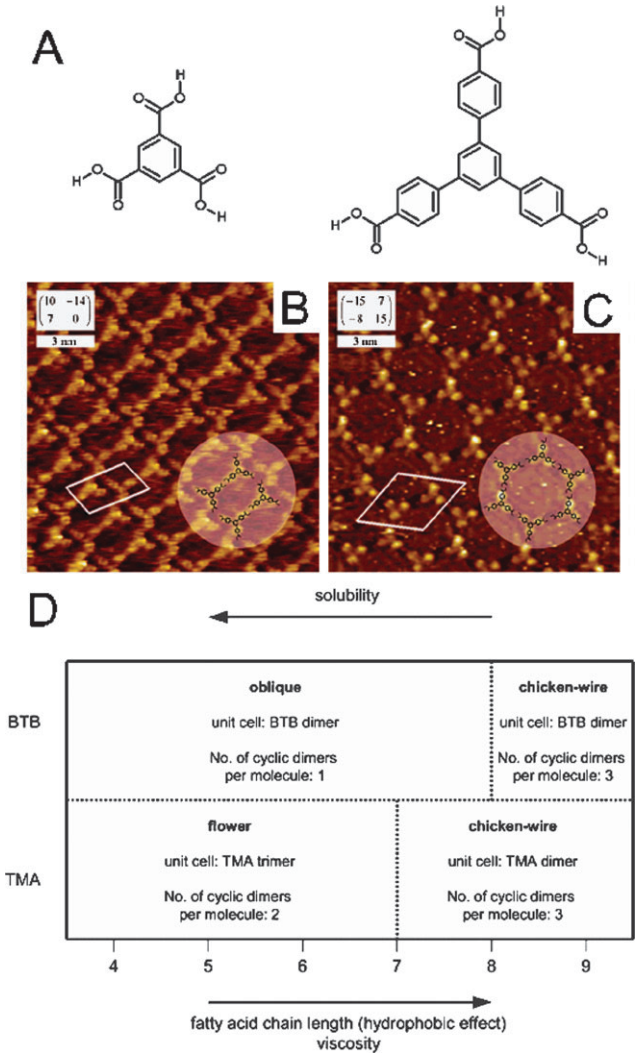

Fig. 13 (A) Molecular structure of TMA and BTB. (B) and (C) STM images of the two polymorphs with oblique and honeycomb unit cell, respectively. (D) Schematic representation of the interfacial structures observed with homogenous alkanoic acids from butanoic to nonanoic acid. (Reproduced with permission from ref. 30. Copyright 2005, American Chemical Society.)

4.2 Control over the structure of 2D nanoporous networks

4.2.1 Solvent control. In addition to adsorbate–adsorbate and adsorbate–substrate interactions, at a solid–liquid interface also the interplay between adsorbates and solvent molecules and interactions between the solvent and the substrate can have a crucial influence on the final outcome of the 2D surface assembly. A typical example of this influence is the solvent-controlled organisation of TMA molecules into various types of nanoporous networks. As mentioned before, TMA molecules can self-assemble into coexisting "flower" and "honeycomb" phases in UHV at a graphite surface (see Fig. 6). Using a homologous series of alkanoic acids, ranging from butyric to nonanoic acid, the dependence of these polymorphs on the solvent was investigated at the liquid–graphite interface.[30]

The solvent appeared to have a significant influence on the structure of the assembly formed by TMA. While in the case of solvents with longer alkyl chains, such as heptanoic, octanoic and nonanoic acid, the honeycomb phase was found, in butyric, pentanoic and hexanoic acid the flower phase was exclusively formed (Fig. 13D). At the graphite/heptanoic acid interface a coexistence of the two phases was observed. Inspection of the STM images (Fig. 6) revealed that the two polymorphs exhibit a 30% difference in molecular packing density, and simple concentration measurements showed an increased solubility of TMA upon a decrease in chain length of the alkanoic acid solvent. Based on these findings, two possible mechanisms for the observed solvent-induced polymorphism were proposed: (i) stabilisation of a specific basic precursor seed unit, that occurs already in solution, by a particular solvent, and (ii) solvent coadsorption and/or stabilisation of the polymorphs on the surface itself. Regarding the first proposed mechanism, the interactions between the carboxylic acid functions within the two polymorphs should be considered. In the case of the honeycomb structure, hydrogen bonded carboxylic acid dimers are the exclusively occurring motifs, whereas in the case of the more closely packed flower structure also hydrogen bonded trimers are present. Taking this into account, the solvents with shorter alkyl chains were proposed to favour the formation of trimer precursors, whereas the solvents with longer alkyl chains favour dimers. Although there was no direct evidence found for

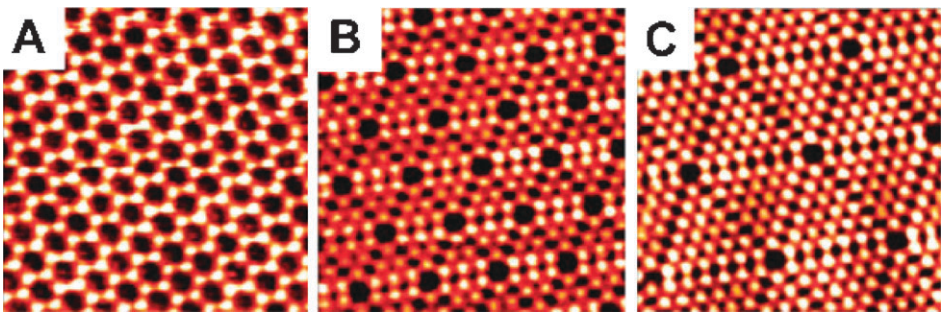

Fig. 14 Coverage induced evolution of TMA assembling structures on a reconstructed Au(111) surface under UHV conditions. (A) Represents the honeycomb structure and (B) and (C) represent two "super-flower" structures of different generation observed at higher surface coverage. (Reproduced with permission from ref. 32. Copyright 2007, American Chemical Society.)

the presence of these precursors, it was suggested that viscosity is one of the factors that influences the equilibrium between TMA dimers and trimers. Regarding the second proposed mechanism, it was rationalised that the smaller solvent molecules may fill the small voids that are present in the flower structure and thereby stabilise it.

Solvent-dependent polymorphs were also observed for an extended analogue of TMA, 1,3,5-benzenetribenzoic acid (BTB),[31] which demonstrates that the influence of solvents on the formation of porous networks is a commonly occurring phenomenon. At the graphite–liquid interface, BTB self-assembles into two non-densely packed polymorphs, depending on the alkyl chain length of the solvent (Fig. 13B and C). Similar as in the case of TMA, these polymorphs differ in their molecular packing density and their hydrogen bonding motifs. A difference with the two polymorphs of TMA, which both have a three-fold symmetry, is the fact that for BTB either an oblique or hexagonal unit cell was observed. Concomitantly, porous networks are formed with either rectangular or circular cavities. The use of butanoic, pentanoic, hexanoic and heptanoic acid, 1-octanol, 1-nonanol and 1-decanol leads to a surface pattern with an oblique unit cell (Fig. 13B), while nonanoic acid and 1-phenyloctane exclusively give honeycomb patterns with cavities of about 2.8 nm in diameter (Fig. 13C). For the solvents octanoic acid and dodecane, a coexistence of both polymorphs was observed. When the occurrence of the different polymorphs was related to the nature of the solvents, a rough dependence on their dielectric constant (ε) could be found. For ε = 3–10, the oblique structure is observed exclusively, whereas for $\varepsilon \leq 2.5$ the honeycomb structure is preferred. However, a different solubility of BTB in these solvents was also noticed, following the same trend as observed for TMA, which means that the possibility that concentration plays a certain role can not be ruled out. Such concentration effects will be further discussed in section 4.2.3.

4.2.2 Surface coverage-control. Although the honeycomb and the flower-structure are the most commonly observed

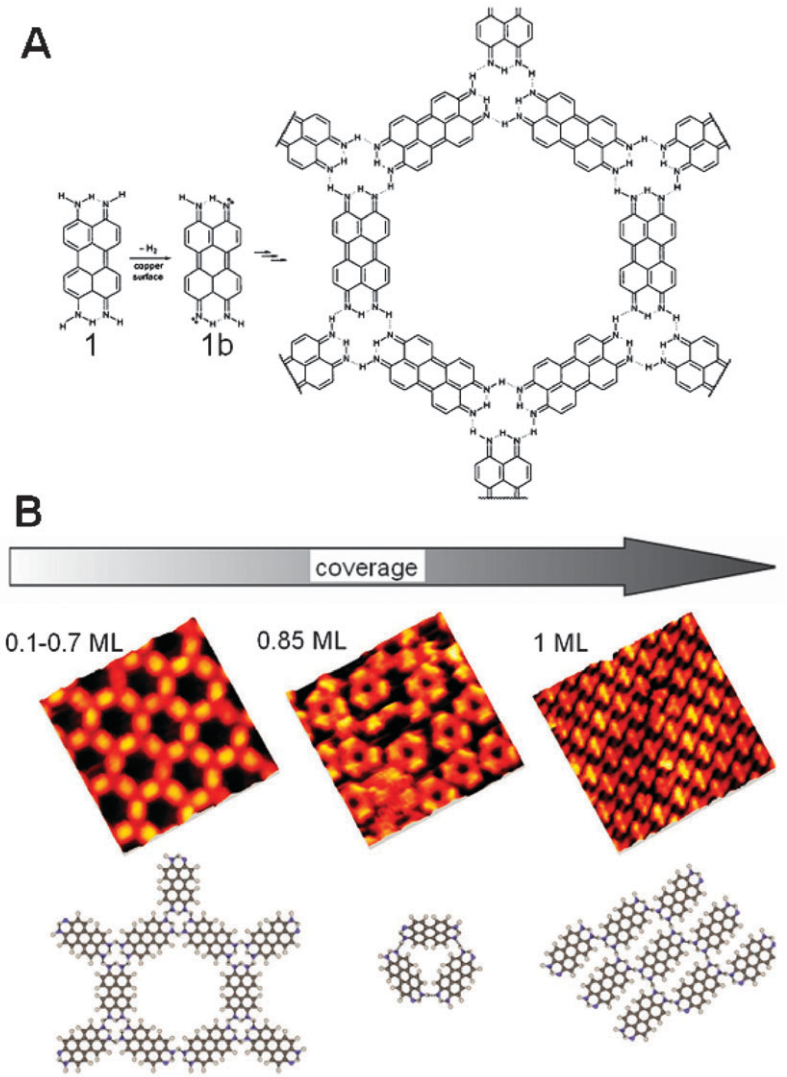

Fig. 15 (A) Thermal generation and hexagonal assembly of thermally generated **1b** on a Cu(111) surface. (B) STM images and the corresponding chemical structures of the surface aggregates at variable coverage of **1b**. (Reproduced with permission from ref. 33. Copyright Wiley-VCH Verlag GmbH and Co. KGaA.)

arrangements observed for TMA on several substrates and under various conditions, a series of other, novel polymorphs could also be induced by increasing the surface coverage of these molecules at a Au(111) surface in UHV.[32] Based on exclusive trimeric hydrogen bonding motifs, at a very high surface coverage a densely packed hexagonal "super flower" structure can be obtained, whereas the open honeycomb structure is the low coverage extreme (Fig. 14). TMA starts to assemble into the honeycomb structure when more than 0.30 monolayer (ML) of the molecule is sublimated onto the surface. A sequential and controlled increase in TMA surface coverage then leads to the appearance of the flower structure and subsequently a series of novel polymorphs, until the most densely packed super flower structure is formed. In this way, also the distance between the pores can be carefully tuned with steps of 0.93 nm. It should be noted that at high surface coverages the self-assembled structures become more sensitive to changes in coverage, resulting in the occurrence of combinations of polymorphs due to local coverage fluctuations.

Surface coverage control over 2D networks has also been demonstrated for a hydrogen bonded system in which 4,9-diaminoperylenequinone-3,10-diimine (DPDI) was used as the building block.[33] Upon thermal deposition of 0.7 ML onto a Cu(111) surface, no ordered arrangement of these molecules was found due to their poor hydrogen bonding donor properties. However, after annealing at 300 °C, a highly ordered honeycomb structure was revealed both by STM and low-energy electron diffraction (LEED) (Fig. 15B). Its formation was rationalised by dehydrogenation of the DPDI monomers on the copper surface during the annealing process, which provides an auto-complementary compound with a quinoidal redox state (Fig. 15A). The network exhibits an extraordinary stability, which is reflected by its inertness toward manipulation with the STM tip and by its thermostability up to 450 °C. This high stability was attributed to a combination of resonance-assisted hydrogen bonding and strong interactions between the molecules and the copper substrate. Upon increasing the surface coverage to 0.85 ML, trimeric structures in the form of rings were generated (Fig. 15B), in which, despite the higher surface packing density, the intermolecular interactions are weaker and the 2D structure is not as robust as the honeycomb one. Upon a further increase in surface coverage to 1 ML, a densely packed and highly ordered molecular array was formed in which each monomer is linked by hydrogen bonds to four adjacent monomers (Fig. 15B).

4.2.3 Concentration control. So far, already many factors that can influence the outcome of a surface-confined self-assembled structure have been discussed. Surprisingly, however, the effect of solute concentration, which is well-known to affect the self-assembled structure of chemisorbed systems such as thiols, has only very recently been noticed and investigated in a systematical fashion in the case of physisorbed systems. At the graphite/TCB interface, alkoxylated DBAs (see Fig. 11) have been reported to form 2D porous networks if their alkoxy chains are shorter than twelve carbon atoms.[28] DBAs with longer alkoxy chains preferably self-assemble into close-packed linear structures. However, it turned out that by tuning the DBA concentration in solution,

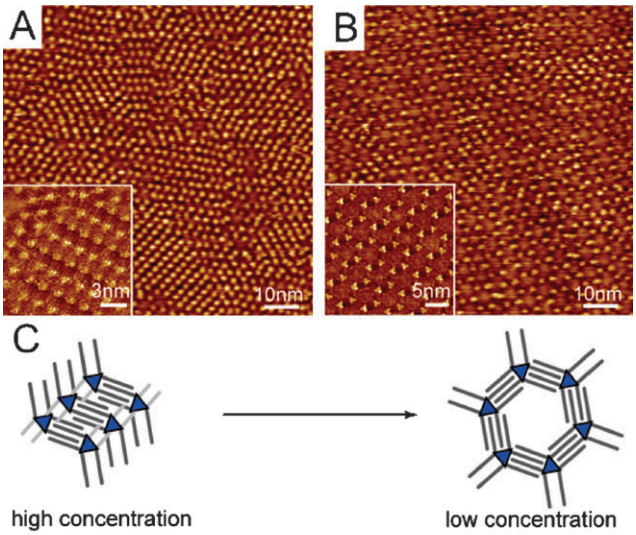

Fig. 16 (A) and (B) STM images obtained at the TCB/graphite interface at DBA-OC16 concentrations of 1.1×10^{-4} mol L^{-1} (V_{bias} = 1.01 V, I_{set} = 220 pA) and 5.7×10^{-6} mol L^{-1} (V_{bias} = 0.80 V, I_{set} = 170 pA), respectively. Insets in (A) and (B) are high resolution images of linear and honeycomb patterns, respectively. (C) Scheme illustrating the structure and the transition of linear-type to honeycomb-type patterns. (Reproduced with permission from ref. 34. Copyright Wiley-VCH Verlag GmbH and Co. KGaA.)

the ratio of both polymorphs can be controlled: either a regular 2D porous honeycomb network is formed at low concentrations, or a densely-packed linear network at high concentrations (Fig. 16).[34] The concentration dependency of both polymorphs has been probed systematically and it was revealed that by applying the so-called 'concentration-in-control' concept, nanoporous networks can be formed of which the pore size is determined by the length of the alkyl chains and can be tuned from 2.9 to 5.4 nm with increments of ~0.4 nm. The influence of concentration on the surface ratio of the polymorphs was modelled, assuming that the adsorption–desorption equilibrium is under thermodynamic control. It turned out that the solute concentration is directly related to the difference in stability between the linear and the honeycomb polymorphs and their respective molecular densities, which could be determined experimentally according to the proposed model. The longer the alkyl chains of the DBA derivatives, the more sensitive becomes the surface coverage of the porous honeycomb structures to the concentration of the building blocks.

4.2.4 Self-repair. Self-recognition, self-selection, self-repair and dynamic self-(re)organisation are key factors of supramolecular self-assembly. With regards to understanding them it is of fundamental importance to get insight in these factors on the molecular level, and studying them at a surface with STM can provide valuable information.

Elegant model systems to study such dynamic processes have proven to be self-assembled Metal-Organic Coordination Networks (MOCNs), which provide a novel route towards porous materials that may find applications in molecular recognition, catalysis, gas storage and separation. One of the

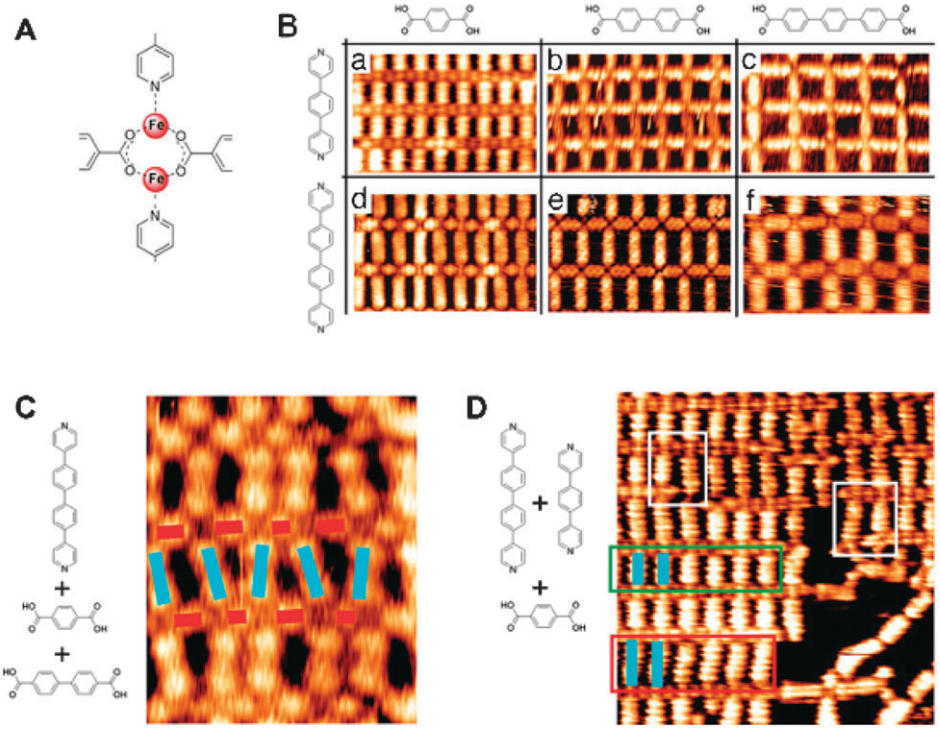

Fig. 17 (A) The coordination motif in networks composed of Fe-atoms, pyridine and carboxylic acid ligands. (B) UHV STM images (9.4 × 6.0 nm) of networks formed by the co-assembly of Fe-atoms with six possible combinations of bipyridine and bis-carboxylic acid ligands; structure periodicities are (a) 1.1 × 1.8 nm, (b) 1.5 × 1.8 nm, (c) 1.8 × 1.8 nm, (d) 1.1 × 2.3 nm, (e) 1.5 × 2.3 nm, (f) 1.8 × 2.3 nm. (C) UHV STM image (6.0 × 9.6 nm) of a distorted network composed from the co-assembly of Fe-atoms and a ternary mixture of one bipyridine and two different bis-carboxylic acid ligands. (D) UHV STM image (14 × 14 nm) of a network composed from the co-assembly of Fe-atoms and a ternary mixture of one bis-carboxylic acid and two different bipyridine ligands. (Reproduced with permission from ref. 35. Copyright 2007, National Academy of Sciences.)

examples of such a MOCN is based on linear polyaromatic bis-carboxylic acids, bipyridines, and Fe-atoms on a Cu(100) surface under UHV conditions.[35] Earlier work had demonstrated that ligands, which contain a carboxyl group on one end and a pyridine group at the other, coordinate to Fe-dimers in a geometry shown in Fig. 17A, in which the two Fe-atoms bridge between two carboxylates and the pyridine groups bind axially. This specific type of coordination self-assembly was used to investigate the nature of the self-assembled structures of a library containing two different bipyridine ligands and three different bis-carboxylic acids (Fig. 17B). The co-deposition of each of the combinations of the ligands together with Fe-atoms yields highly regular porous networks, in which the internal dimensions of the compartments can be tuned by choosing the ligands of the appropriate length. Notably, the 'horizontal rows' all consist of the dicarboxylates, while the 'vertical pillars' are formed by the bipyridines. This type of robust and well-defined self-assembly is a good basis for investigating dynamics of the system and in particular self-sorting and self-repair. These factors are perfectly illustrated when the co-deposition of a ternary combination of one bipyridine ligand and two carboxylic acids is studied (Fig. 17C). Small domains of a distorted network were obtained, indicating a low level of structural accomplishment which did not improve upon thermal annealing. The bis-carboxylates are randomly distributed over the 'horizontal rows', and the pillaring bipyridine ligands adapt themselves to this random sequence by tilting their angles. This 'error-toleration', and the failure of the system to reach thermodynamic equilibrium in the form of stable, phase-separated networks, finds its cause in the high stability of the Fe-carboxylate coordination bonds, which dictates the final arrangement of the components within the metastable structure, with respect to the rather labile axial Fe-pyridine interaction. Significantly improved self-repair is observed when the ternary mixture of components is changed so that it contained two of the more labile bipyridine ligands and one bis-carboxylic acid (Fig. 17D). In this case, networks of well-ordered rectangular compartments are obtained in which local phase separation has taken place to form sub-domains of distinct heteroligand combinations. Within these sub-domains, the pillars are formed by only bipyridine ligands of uniform length. These observations must imply that the self-assembly of the mixture involves both self-selection and self-recognition. Of critical importance to these processes is the possibility of self-repair, which in this mixture relies on a reversible coordination of the bipyridine ligands.

5. Host–guest properties of 2D nanoporous networks

5.1 Binding of guests

An important property, and so far also the main application of 2D nanoporous networks, is the immobilisation of potentially functional guest molecules in a repetitive and spatially ordered

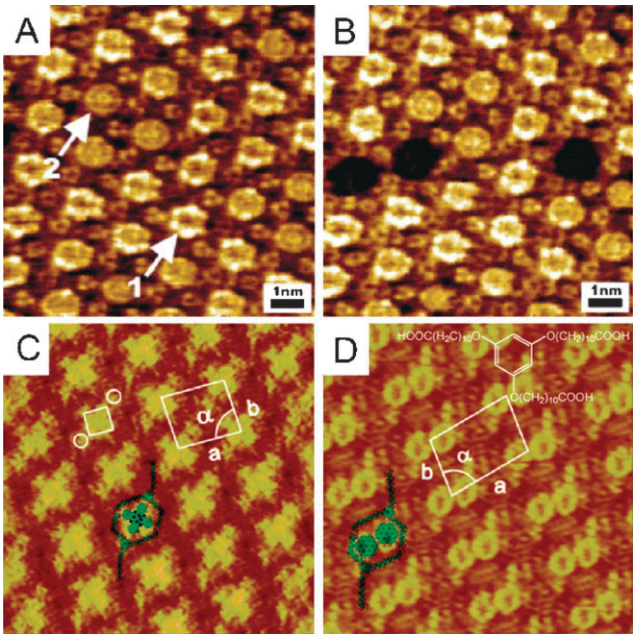

Fig. 18 (A) STM image of coronene in a TMA network showing two different types of contrast as marked by 1 and 2. (B) The same area after removal of some guest molecules. (Reproduced with permission from ref. 36. Copyright 2004 American Chemical Society.) (C) STM image of the CuPc/TCDB guest–host architecture. (D) STM image of the coronene dimers trapped in the TCDB network. The chemical structure of TCDB is overlaid in (D). (Reproduced with permission from ref. 22. Copyright 2004, American Chemical Society.)

arrangement. For example, the honeycomb network formed by TMA has hexagonal cavities with a diameter of 1.1 nm and is highly robust towards disturbances like scanning or manipulation with the STM tip. As such, it can serve as an ideal matrix to study the dynamics of guest binding and manipulation.[36] Upon the addition of a solution containing coronene (Fig. 21), a molecule with a size and shape that is commensurate with the pores, an ordered binary architecture was formed in which each of the cavities was filled with a coronene molecule (Fig. 18A). The perfect host–guest fit is highlighted by the fact that submolecular details of the guest could be revealed by STM, which indicates its strong immobilisation. It was also demonstrated that an increased interaction with the STM tip could temporarily vacate the cavities of the host network (Fig. 18B), followed by a re-occupation by the guests from the liquid phase reservoir.

On a graphite surface, the previously mentioned extended TMA analogue TCDB forms under ambient (dry) conditions 2D hydrogen bonded networks with tetragonal cavities with an inner size of 2.3 × 1.3 nm, which are embraced by four arms of two oppositely positioned TCDB molecules.[22] In contrast to the rigid TMA building block, the flexibility of the alkyl chains of TCDB makes the network more flexible and enables it to adjust its geometry to the included guests. Upon the addition of copper phthalocyanine (CuPc) molecules, these were trapped as guests in the cavities of the TCDB networks to form highly uniform host–guest arrays, and their inclusion induced a significant change in the structure of the network (Fig. 18C). When coronene was used as a guest, two different host–guest architectures were formed, one in which each cavity contained one guest, and another in which coronene dimers were bound. Unlike in the case of one coronene per cavity, in the case of the coronene dimers submolecular features of the guests could be resolved, indicating its total immobilisation in the cavity (Fig. 18D). The unit cells of the host–guest network were significantly smaller than those of the network of the free hosts, which was attributed to stabilising van der Waals interactions between the guests and the side-walls of the hosts.

The flexibility of the TCDB network is an excellent example of how the self-assembled nature of a nanoporous network can be used as a powerful feature to adjust pore size and shape in order to create the ideal confined space for a desired guest. This propensity of pore adjustment, however, is strongly dependent on the nature of the host matrix molecules and the strength and directionality of the supramolecular interactions involved. When these interactions are relatively weak, there is a significant risk that intrinsic instabilities within an open nanoporous network cause a collapse of the porous structure. However, there is an example known in which a

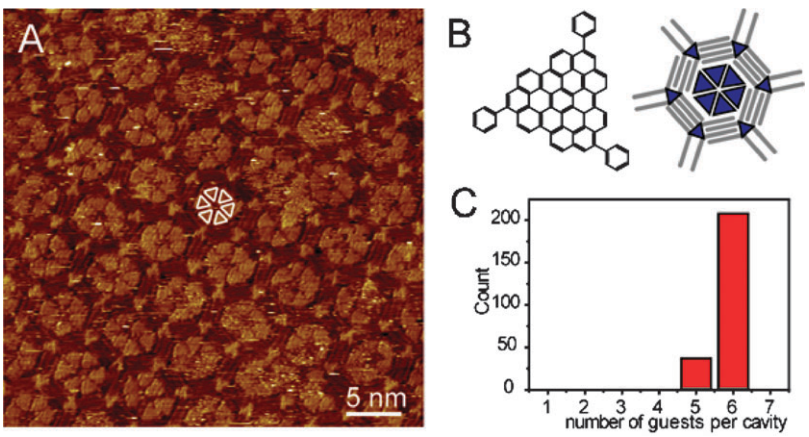

Fig. 19 (A) Host–guest architecture formed by DBA-OC20 with a large nanographene guest. (B) Chemical structure of the large nanographene molecule and a schematic model of the host–guest architecture. (C) Distribution of the number of guests in each cavity. (Reproduced with permission from ref. 38. Copyright 2008, American Chemical Society.)

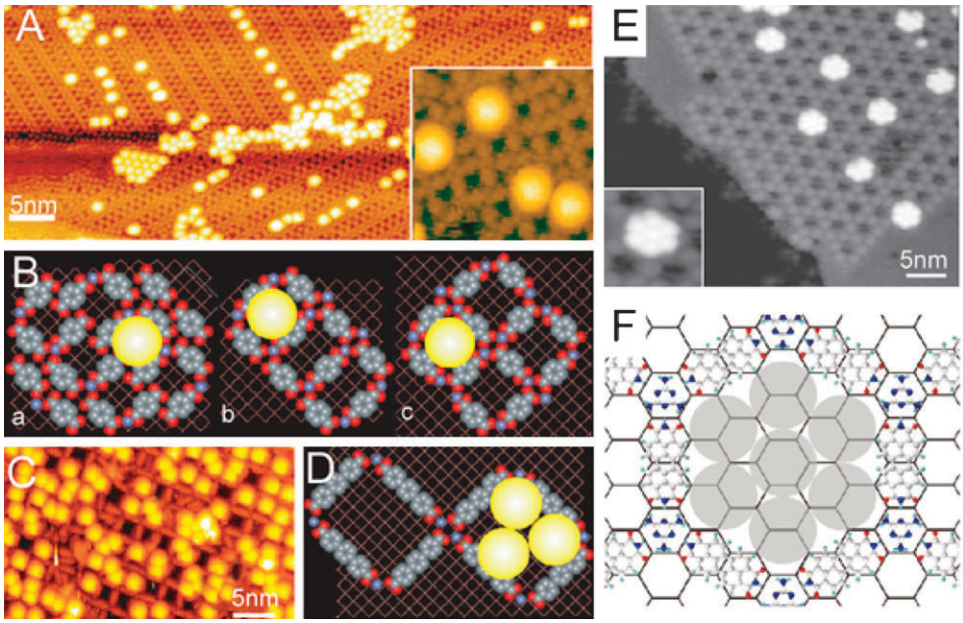

Fig. 20 (A) Adsorption of single C_{60} in Fe-TPA networks. The ladder-type MOCN accounts for linear arrangements of single C_{60} with preferential occupation of the larger cavities. Inset shows C_{60} monomers accommodated in square cavities. (B) Top-view model of C_{60} adsorption in different types of cavities in Fe-TPA networks. (C) STM image of C_{60} accommodated in the mesoscale cavities formed by Fe-TDA, monomers, dimers or trimers can be hosted. (D) Model of Fe-TDA rectangular cavity and accommodation of a C_{60} trimer. (Reproduced with permission from ref. 39. Copyright 2004, Nature Publishing Group.) (E) STM image of C_{60} heptamers trapped in a PTCDI-melamine network, inset: high resolution view of an individual cluster. (F) Schematic model of a C_{60} heptamer. (Reproduced with permission from ref. 23. Copyright 2003, Nature Publishing Group.)

densely packed, stable surface structure could be transformed into a nanoporous network upon the introduction of a proper guest. As was demonstrated before, alkoxylated DBA molecules form either densely packed linear structures or open honeycomb networks, depending on the length of the alkoxy chains and the concentration (see Fig. 11 and 16). The energy differences between these surface structures are not very high, and it was discovered that the addition of coronene to a surface, which was covered by a densely packed structure of DBA-OC14, transformed the arrangement of the host matrix molecules into a honeycomb network in which the guests are bound in the cavities.[37] By increasing the ratio between coronene and DBA, the gradual transformation could be clearly followed by STM, and at a ratio of 7 : 1 nearly the entire surface was covered with the honeycomb domains. Remarkably, such a complete conversion of the network structure only succeeded when DBA-OC14 was used as the hosting molecule. For DBAs with longer alkoxy chains, always a coexistence of linear and honeycomb patterns was observed, even in the presence of a large excess (10 equivalents) of coronene. The structural transformation was explained by an energy gain resulting from molecule–substrate interactions between the physisorbed hosts and guests and the graphite surface, which overcomes the instability related to the formation of voids and the lower density of the host matrix when compared to a densely packed linear structure. This means that in the case of the DBAs with longer alkoxy chains, a guest with stronger adsorption energy than coronene might induce a more complete conversion to a honeycomb network. Indeed, large 'nanographenes' (see Fig. 19), guest molecules with a high affinity for graphite, were found to convert densely-packed linear networks of DBAs with the longest alkoxy chains ($OC_{20}H_{41}$) into honeycomb networks, even at low guest/host ratios.[38] Pore sizes up to 5.4 nm were observed and, depending on the pore size, amounts of one up to maximal six guest molecules could be trapped. Because of the relatively weak intermolecular interactions between the interdigitating alkyl chains, the host matrix was capable of changing its structure in order to accommodate the guest clusters, and as a result of this flexibility the number of guests bound in each cavity always displays a distribution.

Alternatively, the pore shape and size of a nanoporous network can be adapted in a controlled fashion by means of a rationally designed use of the building blocks of the host matrix. As previously mentioned, MOCNs are ideal systems to investigate such an approach (see Fig. 17). Upon their deposition at a Cu(100) surface at room temperature in UHV, the building blocks terephthalic acid (TPA), trimellitic acid (TMLA) and 4,1′,4′,1″-terphenyl-1,4″-dicarboxylic acid (TDA) were found to undergo complexation with coadsorbed Fe atoms, and as a result MOCNs comprising nanometer-sized cavities were formed (Fig. 20).[39] The cavity dimensions could be tuned by using linker molecules with different backbone lengths (~7 Å for TPA and TMLA and ~15 Å for TDA), or by adjusting the coverage of Fe atoms. Depending on the latter and using TPA as a building block, either ladder-type structures with elongated cavities or square reticulations with cross-shaped cavities were formed (Fig. 20A). In the ladder-type structure two different types of elongated cavities

were present, of which according to STM only the larger ones could serve as binding sites for guests such as C_{60}. The square cavities formed at high Fe-coverages could also bind monomers of C_{60}. Although TMLA has an extra carboxyl group pointing towards the inside of the cavity in the network, the MOCN composed of TMLA and Fe shows similar host–guest behaviour toward C_{60}, which indicates that reactive side groups do not influence the adsorption sites. The size of the cavities formed by TDA is larger than the size of C_{60}, and as a result these cavities can host monomers, dimers or trimers of these guests, which could be observed simultaneously (Fig. 20C). The reversibility and strength of the interactions between the cavity and the bound C_{60}-molecules were tested by thermal annealing. Upon exceeding a threshold temperature of 370 K, the C_{60}-molecules were rejected from the Fe-TPA cavities, while for Fe-TDA cavities a temperature higher than 500 K was required. This effect was attributed to the presence of enhanced interactions between the substrate and guest in the latter network, as a result of the larger cavity which allowed their direct contact. Although the Fe-TMLA network exhibited similar host–guest behaviour, the stability of the complexes appeared to be higher, since no release of C_{60} was observed up to 420 K. The apparently increased binding strength indicates that the additional carboxyl group of TMLA significantly modifies the chemical properties of the nanocavities.

A similar ability to organise well-defined clusters of C_{60} in a predefined template has been demonstrated by the previously discussed PTCDI/melamine network (see Fig. 7).[23] The open areas in this network are rather large in comparison with the size of the building blocks, and have been found to serve as traps or vessels for large guest molecules. For example, when 0.03 ML of C_{60} was sublimed onto the network, well-defined heptameric clusters of the guest were formed within the cavities (Fig. 20E). Within the clusters, the C_{60} molecules are hexagonally arranged and a remarkable alignment of clusters in different pores along the principle axes of the Si(111) surface was observed. An increase in C_{60} coverage resulted in the increase of the fraction of pores filled with C_{60} heptamers, finally leading to formation of a termination layer in which C_{60} molecules are located directly on top of the PTCDI and melamine molecules of the network.

The binding of two or multiple guests in one cavity is highly appealing when considering the possibility to use nanoporous networks as functional 2D surfaces covered with nanoscale reaction vessels. Spatial confinement as a strategy to achieve control over the chemical reactivity of organic molecules has been thoroughly employed in solution and in the solid state, exploiting discrete spaces. This approach has been referred to as "cavity-directed synthesis", in which the geometric constraints imposed by the confined space control the complexation and subsequent chemical transformation of bound guest molecules. Such geometrical constraints force the guest molecules into adopting specific conformations and to react in a selective and specific way with its neighbour(s). The highly regular 2D porous networks discussed above arise the possibility to transfer the space-confinement approach exploited in solution or in the bulk solid state to the basal plane of a solid surface, and in conjunction with STM it will allow a real-time investigation of such process at a submolecular scale.

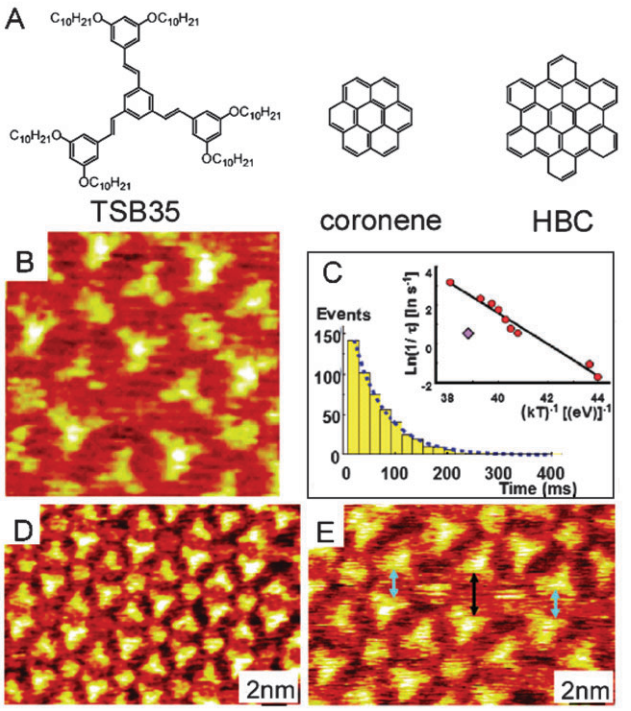

Fig. 21 (A) Chemical structures of TSB35, coronene and HBC. (B) STM image (11 × 11 nm^2) of a TSB35 matrix filled with coronene obtained with a fast scanning speed. (C) Histogram represents the decay of the presence of a coronene molecule as derived from a series of successive images. The inset shows the temperature dependence of the decay constant at the solid–liquid interface (disk) in comparison to that measured under vacuum at room temperature (diamond). The solid line represents an Arrhenius law with an energy barrier of 0.81 ± 0.05 eV. (D) Incompletely filled matrix with under-stoichiometric concentrations of HBC at sample temperature of 22 °C. (E) STM image showing a defect where the distance between two neighbouring TSB35 molecules is increased by 50%. Motion of a HBC molecule between the two adjacent sites was observed. (Reproduced with permission from ref. 40. Copyright 2006, American Chemical Society.)

5.2 Dynamic behaviour and manipulation of guests—towards functional surfaces

One of the advantages of a 2D host–guest system is that it confines individual molecules or molecular clusters to a well-defined environment, which enables addressing them in-situ at the single molecule scale with STM. In this way, dynamic behaviour like the lateral or rotational mobility of guest molecules inside a cavity and hopping between cavities can be investigated, as well as their controlled manipulation by external stimuli such as an STM tip.

At the interface of graphite and 1-phenyloctane, 1,3,5-tris-[(*E*)-2-(3,5-didecyloxyphenyl)ethenyl]benzene (TSB35) self-assembles into a honeycomb network with cavities of ~1.3 nm diameter in size (Fig. 21).[40] The network was found to behave as a "2D molecular sieve" for large aromatic guest molecules such as coronene and hexabenzocoronene (HBC). In the case of both guests, their addition to the subphase

resulted in the appearance of a circular bright spot in the centre of each of the cavities.

The possible diffusion of coronene guests between the cavities in the host matrix was tested at different substrate temperatures. For this purpose, a diluted sub-stoichiometric solution was used to generate an incompletely filled matrix, so that the diffusion of guests from cavity to cavity was allowed, and by applying a fast scanning speed, this diffusion could be reliably traced with STM (Fig. 21B). For each temperature in the range of -9 to $+32$ °C, histograms of residence times were constructed by analysing a series of STM images (Fig. 21C). Exponential decays were obtained of which the characteristic time constants increased with decreasing temperature from 40 ms to 5000 ms. Although there also exists a possibility that guests are not hopping in-plane but simply exchange with guests that are present in solution, there is strong evidence that this does not occur: (i) the two mechanisms should obey different laws of statistics, and the statistics based on the STM observations clearly agree with the hopping mechanism, (ii) in UHV, where no subphase is present, the same in-plane hopping occurs, and (iii) the energy barrier obtained from the fitting of the experimental data, taking into account Arrhenius' law, amounts to $\sim$0.8 eV, which is apparently lower than the desorption energy of coronene from the graphite surface (1.4 eV).

In contrast to coronene, HBC guests remain bound in the network at any scanning rates and temperatures up to 47 °C. Interestingly, by coincidence a defect consisting of a $\sim$50% increased spacing between two neighbouring matrix molecules was observed. The contents of the cavities on either side of this wider channel appear striped, and the two sets of stripes are anti-correlated, which means that during each scan the HBC guest is observed in either one cavity or the other. This observation strongly indicates that hopping is easier through the densely packed alkyl moieties than through the conjugated cores, which means that the spaces between these cores can serve as a channel for transport of the guest molecules. Only guests with sizes smaller than the channel can diffuse between the cavities, which makes the TSB35 matrices represent a 2D analogue of molecular sieve.

Besides hopping between cavities of a host matrix, another interesting form of dynamical behaviour is the rotation of a guest inside a cavity. When a host matrix is highly regular, it is possible to address each bound guest by labelling its position within the network and determining its arrangement with respect to the network and the STM scanning direction.

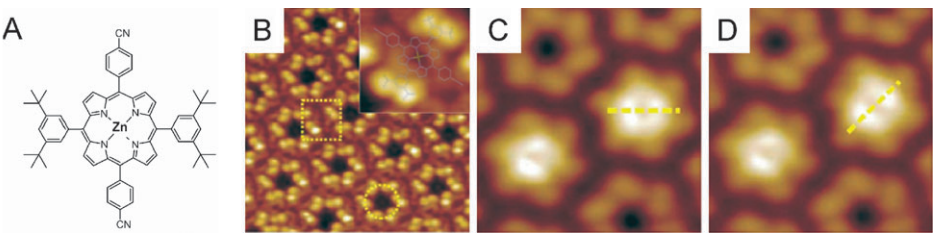

Fig. 22 (A) Structure of the porphyrin. (B) STM image (12.5 × 12.5 nm^2) of a self-assembled network of a porphyrin derivative on a Cu(111) surface. Inset is close view of a single molecule and a molecular model is overlaid. (C) and (D): STM images (6.5 × 6.5 nm^2) recorded before and after switching of an individual guest molecule, respectively. (Reproduced with permission from ref. 41. Copyright Wiley-VCH Verlag GmbH and Co. KGaA.)

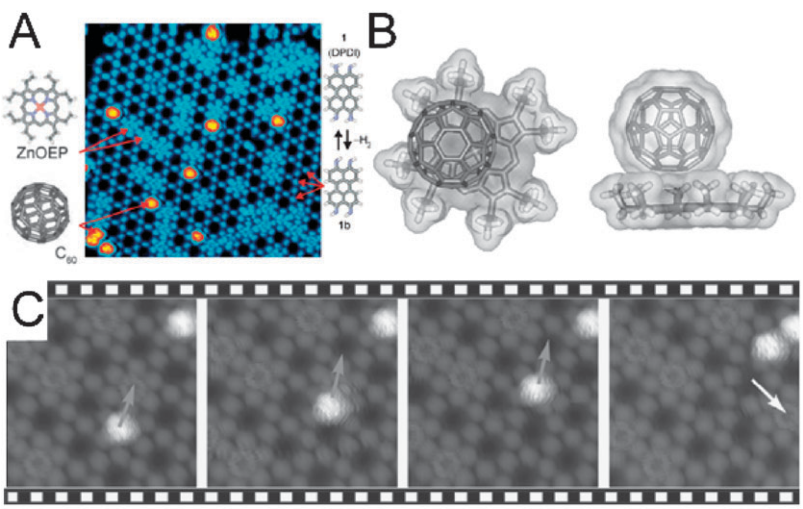

Fig. 23 (A) STM image (30 × 30 nm^2) (middle) of C_{60} and ZnOEP trapped in the honeycomb network formed by dehydro-DPDI (**1b**). The chemical structure of ZnOEP and C_{60} (left), and thermal generation of **1b** (right) are also shown. The chemical structures are assigned to the molecular units by arrows. (B) Side- and top-view model of C_{60} placed on top of a ZnOEP molecule. The C_{60} molecule occupies a slightly off-centre position. (C) A sequence of STM images (20 × 20 nm^2) displaying the vertical manipulation of an individual C_{60} molecule. (Reproduced with permission from ref. 42. Copyright Wiley-VCH Verlag GmbH and Co. KGaA.)

At a Cu(111) surface, the porphyrin derivative shown in Fig. 22A self-assembles into a regular nanoporous network as a result of weak hydrogen bonding between the phenyl ring and the cyano residues (Fig. 22B).[41] Each of the cavities of the network is surrounded by six flat lying porphyrins, with each porphyrin acting as side-wall of two neighbouring pores. The arrangement of the porphyrins around the pores has a chiral nature, and both types of homochiral domains were observed in the experiments. Interestingly, the molecule could be self-trapped on top of the pores. In that way it makes no contact with the substrate, and it can rotate freely between six possible orientations, which makes it a single molecule rotation device (Fig. 22C). The rotation speed was found to depend on the temperature, and around 112 K switching events of individual guests between different stable orientations could be monitored by STM. Analysis of successive STM images taken at temperatures between 112 and 116 K allowed the estimation of the switching activation energy, which was determined as being 0.24 ± 0.08 eV. An even more interesting observation was that the individual guest molecules could be selectively addressed and switched by the STM tip. For this purpose, the sample was cooled to 77 K, a temperature where no thermally induced switching occurs. Subsequently, the STM tip was placed above a guest molecule, and by applying a short pulse, single switching events could be triggered with molecular precision, leaving neighbouring guests unaffected (Fig. 22D).

As a final example of manipulating guests in a 2D nanoporous network it will be shown that in one self-assembled system two types of lateral movement of guest molecules is possible. The previously discussed network based on DPDI molecules (see Fig. 15) exhibits in addition to a high structural regularity also an outstanding stability, and therefore it provides an ideal starting point for the construction of functional hierarchical host–guest assemblies. Both C_{60} and zinc octaethyl porphyrin (ZnOEP) molecules could be trapped simultaneously in the network in a statistical distribution (Fig. 23A).[42] At 77 K, C_{60}-molecules do not show any mobility within the cavities, while ZnOEP molecules still exhibit a thermally activated rotation. Because even at room temperature the probability of hopping between cavities is low due to the high-energy barrier set by the cavity walls, the system becomes highly appropriate for controlled lateral manipulation. Two approaches have been utilised to laterally move a trapped C_{60} molecule from one cavity to another. In the first approach, the so-called "constant-height manipulation mode", the feedback system is switched off while the tip is placed above an empty cavity while the C_{60}-molecule to be repositioned is hosted in a neighbouring cavity, whereupon the STM tip is approached 0.40 nm towards the sample surface. The series of STM images in Fig. 23C shows how such a manipulation can be used to fabricate a model system of a ball bearing at the single molecular level. A C_{60} molecule is moved on top of an individual ZnOEP molecule which is trapped in an adjacent cavity. In the resulting complex, the C_{60}-moiety sits in a slightly off-centre position on top of the porphyrin, probably because of preferred π-stacking interactions. This hetero-molecular junction can be envisaged as a solid ball placed onto the porphyrin ring and suspended by the eight ethyl legs (Fig. 23B).

In a second approach, a vertical manipulation was conducted in which the tip is placed directly above a C_{60}-molecule, the feedback loop is turned off, and the tip is approached 0.4 nm toward the surface to pick up a molecule. In case of a successful pick-up, changes in the current and height signals were observed. By positioning the tip above an empty cavity and turning off the feedback, followed by a 0.4 nm approach of the tip toward the surface, the C_{60}-molecule could be placed back to the surface into a desired cavity.

6. Conclusions and outlook

The formation of porous 2D confined networks receives a lot of attention nowadays and it has boosted the research in physisorbed self-assembled molecular systems. Primarily driven by academic curiosity, the research activities have revealed a number of previously unexplored aspects of monolayer formation such as concentration and surface coverage control, self-recognition and self-selection, and the effect of solvents on self-assembly. In general, the research activities targeting the formation of nanoporous structures provide a wealth of insight in the concepts which drive monolayer formation and stabilisation (molecule–molecule, molecule–substrate, molecule–solvent interactions, *etc*.)

Considering the examples of porous 2D surfaces that have been given in this review, it is clear that both approaches to construct them, *i.e*. by using preformed covalently built cavity molecules or by the *in situ* self-assembly of smaller building blocks, can be quite successful. A disadvantage of the covalent approach is not only the time-consuming and generally complex synthesis of the cavity molecules, but, more importantly, its low versatility in the sense that introducing modifications into the molecules is often not straightforward. This is in particular a major handicap when a dynamic tuning of the size of the pores is desired. The self-assembly approach, in contrast, makes use of much smaller molecules that are in general relatively easy to synthesise and modify. The approach, however, does require a careful design of the building blocks so that they self-assemble into a desired 2D structure. Although directional supramolecular interactions, such as hydrogen bonding and metal–ligand interactions, have proven to be quite predictable, other factors that play a role during self-assembly processes, such as entropy and the influence of the solvent and the surface, can be rather elusive and difficult to control.

The main aspect though which makes the field of 2D nanoporous materials 'hot' is the broad range of potential applications. Nanopores can host and immobilise a large variety of guest species. The orientation of the guest species can be determined (visualised), followed in time, or manipulated, reflecting new concepts for data storage. Note that such nanopores can be chiral, which paves the way to enantioselective adsorption of guest molecules in future studies. Nanopores could also act as reaction vessels, *e.g*. for the templated synthesis of inorganic and organic nanoparticles.

Quite some progress has been made in this field which is hardly five years old. Slowly, the nanopores reveal their secrets, both as far as their formation and properties are concerned, but for sure, many more aspects are waiting to be discovered.

Acknowledgements

The authors thank the Inter-University Attraction Pole program of the Belgian Federal Science Policy Office (PAI 6/27) and European Union Marie Curie Research Training Network CHEXTAN (MRTN-CT-2004-512161). T. K., S. L. and J. A. A. W. E. thank the Fund of Scientific Research—Flanders (FWO) and K. U. Leuven for financial support. The authors wish to express their gratitude to their international collaborators in the field of nanoporous networks: Prof. Y. Tobe and Dr K. Tahara (Osaka University), Prof. S. Höger (University of Bonn) and Prof. K. Müllen (Max Planck Institute for Polymer Research, Mainz). A special thanks to Dr Shuhei Furukawa, Dr Hiroshi Uji-i, and Dr Wael Mamdouh who initiated these research activities in Leuven.

References

1 S. De Feyter and F. C. De Schryver, *Chem. Soc. Rev*., 2003, **32**, 139–150.
2 J. M. Lehn, *Supramolecular Chemistry: Concept and Perspectives*, VCH, Weinheim, 1995.
3 A. Ulman, *Chem. Rev*., 1996, **96**, 1533; and references therein.
4 G. Binnig, H. Roher, C. Gerber and E. Weibel, *Phys. Rev. Lett*., 1982, **49**, 57.
5 G. Binnig, C. F. Quate and C. Gerber, *Phys. Rev. Lett*., 1986, **56**, 930.
6 Y. Sambongi, Y. Iko, M. Tanabe, H. Omote, A. Iwamoto-Kihara, I. Ueda, T. Yanagida, Y. Wada and M. Futai, *Science*, 1999, **286**, 1722.
7 H. Seelert, A. Poetsch, N. A. Dencher, A. Engel, H. Stahlberg and D. J. Müller, *Nature*, 2000, **405**, 418–419.
8 S. Scheuring, J. N. Sturgis, V. Prima, A. Bernadac, D. Lévy and J.-L. Rigaud, *Proc. Natl. Acad. Sci. U. S. A*., 2004, **101**, 11293.
9 N. C. Seeman, *Nature*, 2003, **421**, 427; H. Yan, S. H. Park, G. Finkelstein, J. H. Reif and T. H. LaBean, *Science*, 2003, **301**, 1882.
10 Y. He, Y. Chen, H. Liu, A. E. Ribbe and C. Mao, *J. Am. Chem. Soc*., 2005, **127**, 12202.
11 N. Chelyapov, Y. Brun, M. Gopalkrishnan, D. Reishus, B. Shaw and L. Adleman, *J. Am. Chem. Soc*., 2004, **126**, 13924.
12 A. Ohira, M. Sakata, C. Hirayama and M. Kunitake, *Org. Biomol. Chem*., 2003, **1**, 251.
13 S. Yoshimoto, K. Suto, A. Tada, N. Kobayashi and K. Itaya, *J. Am. Chem. Soc*., 2004, **126**, 8020.
14 S. Höger, K. Bonrad, A. Mourran, U. Beginn and M. Möller, *J. Am. Chem. Soc*., 2001, **123**, 5651; D. Mössinger, J. Hornung, S. Lei, S. De Feyter and S. Höger, *Angew. Chem., Int. Ed*., 2007, **46**, 4802.
15 G.-B. Pan, J.-M. Liu, H.-M. Zhang, L.-J. Wan, Q.-Y. Zheng and C.-L. Bai, *Angew. Chem., Int. Ed*., 2003, **42**, 2747.
16 J. Krömer, I. Rios-Carreras, G. Fuhrmann, C. Musch, M. Wunderlin, T. Debaerdemaker, E. Mena-Osteritz and P. Bäuerle, *Angew. Chem., Int. Ed*., 2000, **39**, 3481.
17 E. Mena-Osteritz and P. Bäuerle, *Adv. Mater*., 2006, **18**, 447.
18 J. R. Gong, L. J. Wan, Q. H. Yuan, C. L. Bai, H. Jude and P. J. Stang, *Proc. Natl. Acad. Sci. U. S. A*., 2005, **102**, 971.
19 C. Safarowsky, L. Merz, Alexander Rang, P. Broekmann, B. A. Hermann and C. A. Schalley, *Angew. Chem., Int. Ed*., 2004, **43**, 1291.
20 N. Dmitriev, N. Lin, J. Weckesser, J. V. Barth and K. Kern, *J. Phys. Chem. B*, 2002, **106**, 6907.
21 S. Griessl, M. Lackinger, M. Edelwirth, M. Hietschold and W. M. Heckl, *Single Mol*., 2002, **3**, 25.
22 J. Lu, S. B. Lei, Q. D. Zeng, S. Z. Kang, C. Wang, L. J. Wan and C. L. Bai, *J. Phys. Chem. B*, 2004, **108**, 5161.
23 J. A. Theobald, N. S. Oxtoby, M. A. Phillips, N. R. Champness and P. H. Beton, *Nature*, 2003, **424**, 1029.
24 U. Schlickum, R. Decker, F. Klappenberger, G. Zoppellaro, S. Klyatskaya, M. Ruben, I. Silanes, A. Arnau, K. Kern, H. Brune and J. V. Barth, *Nano Lett*., 2007, **7**, 3813.
25 G. Pawin, K. L. Wong, K.-Y. Kwon and L. Bartels, *Science*, 2006, **313**, 961.
26 H. Spillmann, A. Kiebele, M. Stöhr, T. A. Jung, D. Bonifazi, F. Cheng and F. Diederich, *Adv. Mater*., 2006, **18**, 275.
27 S. Furukawa, H. Uji-i, K. Tahara, T. Ichikawa, M. Sonoda, F. C. De Schryver, Y. Tobe and S. De Feyter, *J. Am. Chem. Soc*., 2006, **128**, 3502.
28 K. Tahara, S. Furukawa, H. Uji-i, T. Uchino, T. Ichikawa, J. Zhang, W. Mamdouh, M. Sonoda, F. C. De Schryver, S. De Feyter and Y. Tobe, *J. Am. Chem. Soc*., 2006, **128**, 16613.
29 M. C. Lensen, K. Takazawa, J. A. A. W. Elemans, C. R. L. P. N. Jeukens, P. C. M. Christianen, J. C. Maan, A. E. Rowan and R. J. M. Nolte, *Chem.–Eur. J*., 2004, **10**, 831; C. R. L. P. N. Jeukens, M. C. Lensen, F. J. P. Wijnen, J. A. A. W. Elemans, P. C. M. Christianen, A. E. Rowan, J. W. Gerritsen, R. J. M. Nolte and J. C. Maan, *Nano Lett*., 2004, **4**, 1401.
30 L. Kampschulte, M. Lackinger, A. K. Maier, R. S. K. Kishore, S. Griessl, M. Schmittel and W. M. Heckl, *J. Phys. Chem. B*, 2006, **110**, 10829.
31 M. Lackinger, S. Griessl, W. M. Heckl, M. Hietschold and G. W. Flynn, *Langmuir*, 2005, **21**, 4984.
32 Y. Ye, W. Sun, Y. Wang, X. Shao, X. Xu, F. Cheng, J. Lim and K. Wu, *J. Phys. Chem. C*, 2007, **111**, 10138.
33 M. Stöhr, M. Wahl, C. H. Galka, T. Riehm, T. A. Jung and L. H. Gade, *Angew. Chem., Int. Ed*., 2005, **44**, 7394.
34 S. Lei, K. Tahara, F. C. De Schryver, M. Van der Auweraer, Y. Tobe and S. De Feyter, *Angew. Chem., Int. Ed*., 2008, **47**, 2964.
35 A. Langner, S. L. Tait, N. Lin, C. Rajadurai, M. Ruben and K. Kern, *Proc. Natl. Acad. Sci. U. S. A*., 2007, **104**, 17927.
36 S. J. H. Griessl, M. Lackinger, F. Jamitzky, T. Markert, M. Hietschold and W.M. Heckl, *Langmuir*, 2004, **20**, 9403.
37 S. Furukawa, K. Tahara, F. C. De Schryver, M. Van der Auweraer, Y. Tobe and S. De Feyter, *Angew. Chem., Int. Ed*., 2007, **46**, 2831.
38 S. Lei, K. Tahara, X. Feng, S. Furukawa, F. C. De Schryver, K. Müllen, Y. Tobe and S. De Feyter, *J. Am. Chem. Soc*., 2008, **130**, 7119.
39 S. Stepanow, M. Lingenfelder, A. Dmitriev, H. Spillmann, E. Delvigne, N. Lin, X. Deng, C. Cai, J. V. Barth and K. Kern, *Nat. Mater*., 2004, **3**, 229.
40 G. Schull, L. Douillard, C. Fiorini-Debuisschert and F. Charra, *Nano Lett*., 2006, **6**, 1360.
41 N. Wintjes, D. Bonifazi, F. Cheng, A. Kiebele, M. Stöhr, T. Jung, H. Spillmann and F. Diederich, *Angew. Chem., Int. Ed*., 2007, **46**, 4089.
42 M. Stöhr, M. Wahl, H. Spillmann, L. H. Gadem and T. A. Jung, *Small*, 2007, **3**, 1336.